STUDY OF THE EFFECT OF ION CONCENTRATION, PH, AND SURFACE CHARGE ON SINGLE-PARTICLE PLACEMENT

by

KUNHUA YU

Presented to the Faculty of the Graduate School of

The University of Texas at Arlington in Partial Fulfillment

of the Requirements

for the Degree of

MASTER OF SCIENCE IN MATERIALS SCIENCE AND ENGINEEING

THE UNIVERSITY OF TEXAS AT ARLINGTON

May 2015

Copyright © by KunHua Yu

All Rights Reserved

Acknowledgements

This thesis could not be completed without the help and support of many people. Here I express my sincere gratitude and deepest respect to all of them. First of all, I will thank my parents ZhenXing Yu and XiaoMei Yu. They provided me with most of financial aid which I needed to get my M.S. degree. And they gave me tremendous confidence and encouragement when I was stressed.

I thank my advisor Dr. Seong Jin Koh, who gave me a very nice project and some financial support to do research. Sometimes, when I encountered the mental block during the experiment, Doc. Koh would furnish me intelligent suggestions and show me a correct way to overcome the mental block. It is no exaggeration to say Doc. Koh inspirited me to become a much more rigorous and diligent researcher.

I would like to thank my group member Manouchehr, Jason, Prodeep, Vinal, Derek being with me the whole way through. They gave me valuable suggestion patiently and cheered me up when my experimental data was not good.

Also, I owe my gratitude to Doc.Kytai, Rechard, Dennis and Kevin. They gave me access to very important experimental devices and teach me how to operate the devices for my experiment.

Lastly, I offer my best regards and blessings to all of those people who helped me during my thesis.

April 17, 2015

Abstract

STUDY OF THE EFFECT OF ION CONCENTRATION, PH, AND SURFACE CHARGE ON SINGLE-PARTICLE PLACEMENT

KunHua Yu, M.S.

The University of Texas at Arlington, 2015

Supervising Professor: Seong Jin Koh

Single particle placement (SPP) in which nanoparticles are placed on exact substrate positions on a single particle level has drawn a lot of attention as it can be used as an effective tool for bottom-up fabrications of nanoscale systems. In SPP, single nanoparticles are electrically guided toward substrate target positions through electrostatic funneling mechanism and once a single nanoparticle is placed on a target position it prevents the other nanoparticles from approaching toward the substrate, leading to placement of exactly one nanoparticle on each target position. This thesis investigates the role of three key parameters on the effectiveness of the SPP. The three parameters are the surface charge of the nanoparticles, ion concentration of the colloidal solution, and the pH of the colloidal solution. These three parameters control the electrostatic interactions between the nanoparticles and the substrate, thereby enabling fine tuning the SPP process.

The SPP was carried out using 30 nm colloidal Au nanoparticles as the model nanoparticles. The electrostatic guiding structure was formed using self-assembled monolayers (SAMs) of 3-aminopropyltriethoxysilane (APTES) and 16-mercaptohexadecanoic acid (MHA) formed on silicon dioxide and Au substrate surfaces, respectively. Circular patterns of APTES-terminated SiO2 were formed on silicon substrate with remaining area covered with MHA-terminated Au surface, with APTES-

terminated circular SiO2 positively charged and MHA-terminated Au surface negatively charged. The electrostatic interaction of negatively-charged Au nanoparticles and the SAMs-modified patterned substrate was investigated with differing diameters of the circular templates under varying conditions of the three key parameters.

The surface charge of the nanoparticle was controlled by attaching DNA molecules to the Au nanoparticles surface. Gold nanoparticle surfaces were loaded with thiol-terminated (H-S-) single-stranded DNA through Au-S chemical bonding. The ion concentration and buffer pH of the colloidal solution were controlled by varying Na_2HPO_4 and NaH_2PO_4 concentrations in DI water. The ion concentrations were varied from 0.01 mM to 0.1 mM with pH fixed at 7.0. pH's were varied from 7.0 to 8.0 with the ion concentration fixed at 0.05 mM.

The effects of the three parameters on the SPP were investigated using varying circular template diameters, ranging from 150 nm to 300 nm. The electrostatic interactions between nanoparticles and the substrate guiding structure prevented single nanoparticles from being placed onto small circular templates and there existed critical diameters below which no particles can enter the circular templates. The SPP occurred at these critical diameters; for smaller diameters, no nanoparticles enter the circular templates and for larger diameters, more than one nanoparticle enter the circular template. The change of critical diameters with change of the three parameters was investigated. When no DNA is loaded on the nanoparticle surface, the Au nanoparticles became aggregated at ion concentration of 0.01 mM, the lowest ion concentration studied in this thesis. With nanoparticles loaded with DNA, the nanoparticle surface charge increased, resulting in zeta potential of -35 mV, which enabled the SPP. For ion concentrations of 0.1 mM, 0.05 mM and 0.01 mM with pH fixed at 7.0, the SPP was enabled with critical diameters of 210 nm, 250 nm and 280 nm, respectively. The

increasing critical diameters with decreasing ion concentrations were attributed to longer ranges of electrostatic interactions between the nanoparticles and substrate surface with increased Debye lengths. For pH of 7.0, 7.5 and 8.0 with the ion concentration fixed at 0.05 mM, the critical diameters were measured as 250 nm, 280 nm and 320 nm, respectively. This was attributed to increasing degree of deprotonation of the carboxyl-terminated MHA SAMs ($-COO^-$) on the patterned Au substrate with increasing pH, leading to more repulsive forces between the nanoparticles and Au patterns. This study showed that the SPP process can be tuned with appropriate combinations of nanoparticle surface charge, ion concentrations of the nanoparticle colloid and the pH of the nanoparticle colloid.

Table of Contents

List of Illustrations

List of Tables

Chapter 1

Introduction

1.1 introduction

Recently, there has been a great interest in fabricating nanoscale systems through the bottom-up construction of nanoscale building blocks, such as nanoparticles [1, 3], nanotubes [4, 6] and nanowires [7, 12]. For the bottom-up fabrication of nanoscale systems, it is important to have the capability of placing the nanoscale building blocks on target substrate positions with nanoscale precision. Many novel methods for accurately placing nanoscale building blocks have been investigated. These include electric-field assisted placement [13, 14], placement of molecules or atoms using scanning tunneling microscopy [15, 16], capillary force assisted [17,18] placement and DNA-assisted placement [19, 20]. The ultimate control of placing nanoscale building blocks would be the capability of placing the building blocks on a single-entity level, *i.e*., the capability of placing exactly one single building block to an exact target location. In addition, for practical applications, the single-entity level placement needs to be carried out on a large scale over an entire substrate.

Recent progress has demonstrated that single nanoparticles can be placed on exact target locations on a single nanoparticle level [21]. In this approach, called single-particle placement (SPP), single nanoparticle are electrostatically guided onto substrate target positions and once a single nanoparticle is positioned on a target position it prevents the approach of other nanoparticles, resulting in self-limiting single-particle level placement. Figure 1-1 shows schematic of the SPP. The electrostatic guiding structure is made by functionalizing the substrate surface with positively- and negatively-charged self-assembled monolayers (SAMs), which are schematically represented in Fig. 1-1 by the blue and yellow surfaces, respectively. When the substrate is immersed into colloidal

solution of nanoparticles (negatively charged), the nanoparticles are electrostatically guided toward the centers (the target positions) of the circular templates and once a single nanoparticle is placed at the circle center, it prevents the approach of other nanoparticles, leading to placement of exactly one nanoparticle per target position. Importantly, the SPP can be carried out on a large scale over a large area as the electrostatic guiding structure can be fabricated using conventional microfabrication techniques involving photolithography.

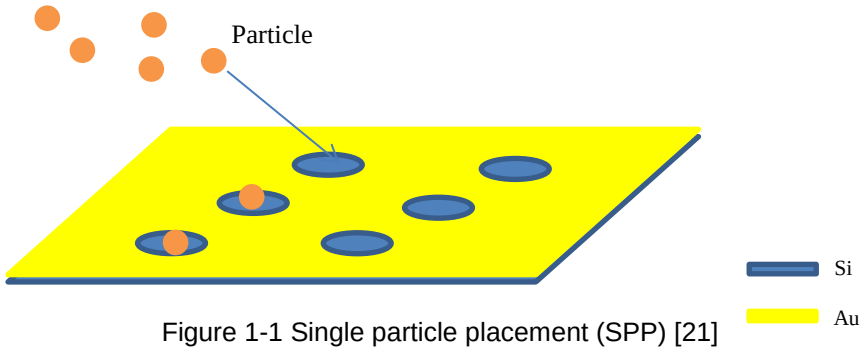

Figure 1-1 Single particle placement (SPP) [21]

The SPP technique can have many practical applications. For example, a practical application for accurately defining transistor contact via holes has been recently demonstrated [22]. Moshood K. Morakinyo and Shankar B. Rananavare have used the SPP technique to reduce the large fluctuation of via hole sizes and line edge roughness which are caused by the intrinsic shot noise in the photolithography of very small patterns (<20 nm). They utilized the SPP to place exactly one single Au nanoparticle accurately on each target position (the via hole location) and the uniform sizes of nanoparticles were used to define via holes with very little size fluctuation. This is just one example that demonstrates the power of the SPP, but it can be envisioned that the SPP can be a vital tool for large-scale bottom-up fabrications of nanoscale systems for many practical applications.

1.2 Motivation and Approach

To maximize the capability of the SPP, it is important to systematically investigate the role of key parameters on the effectiveness of the SPP. This thesis investigates the role of three parameters: 1) surface charge of the nanoparticles, 2) ion strength of the nanoparticle colloid, and 3) pH of the nanoparticle colloid.

The three parameters are controlled as follows. 1) The surface charges are controlled by attaching thiol-terminated (-SH) single-stranded DNA molecules to 30 nm Au nanoparticle surface through the thiol-Au bonding. 2) The ion strengths of the nanoparticle colloids are controlled by selecting the amount NaH_2PO_4 and Na_2HPO_4 in solution. 3) The pH of the nanoparticle colloid is controlled by selecting the ratio of NaH_2PO_4 and Na_2HPO_4 in solution. The effect of the three parameters on the SPP was assessed by observing the SPP for differing sizes of circular templates, with diameters ranging from 150 nm to 300 nm. For this the critical diameter was defined as the diameter of the circular template below which no nanoparticle enters into the circular template. The effects of the three parameters on the SPP were investigated by measuring the critical diameters for differing parameter values.

1.3 Thesis outline

The objective of this thesis is to investigate the roles of the three parameters on the effectiveness of the single particle placement. In Chapter 1, the SPP concept is introduced along with an example of SPP application. Chapter 1 also describes the motivation of the thesis and experimental approaches. Chapter 2 describes the zeta potential, effect of DNA loading, effect of ion concentration and pH. Chapter 3 describes experimental procedure. It includes the method to fabricate electrostatic guiding structure on the template surface as well as the procedure to conjugate the 30 nm Au

nanoparticles with single-stranded DNA molecules. Experiment data are presented in Chapter 4. Chapters 5 presents the conclusions of this thesis.

Chapter 2

Fundamental theory

2.1 introduction

This chapter describes the electrostatic interactions between nanoparticles and substrate surface and the effect of the three parameters on the electrostatic interactions. Calculation of the Debye screening length, which guides the design of the SPP, is also presented.

2.2 Zeta potential

The surface charge of colloidal nanoparticles is screened by ions having the opposite charge and leads to ion distributions schematically shown in Fig. 2-1. The electrostatic potential at the slipping plane in Fig. 2-1 is called the zetal potential (ζ) [23, 28] and it is a good measure to characterize the strength of the surface potential of nanoparticles and the degree of surface charges.

A colloidal solution of nanoparticles contain positive and negative ions. For a negatively charged nanoparticle, positive ions are attracted to the nanoparticle surface to form a compact layer called stern layer, Fig. 2-1. The ions in the stern layer partially screens the negative charge of the nanoparticle surface. Addition positive ions screens the negative surface charges of nanoparticle surface, forming another layer called diffusion layer. These two layers are known as the double layer [29, 33]. When a nanoparticle migrates in a solution, the ions that are close to the nanoparticle surface (therefore relatively well-bounded to the nanoparticle) move together with the nanoparticle, setting a boundary called a slipping plane, Fig. 2-1. The electrostatic potential at the slipping plane is the zeta potential.

The magnitude of zeta potential reflects the stability of a nanoparticle colloid. Nanoparticles with a high zeta potential are stable and do not aggregate, but nanoparticles with a low zeta potential are not stable and can suffer an aggregation. Nanoparticle with a higher zeta potential will have stronger electrostatic interactions between the nanoparticles and also between the nanoparticle and charged substrate surface.

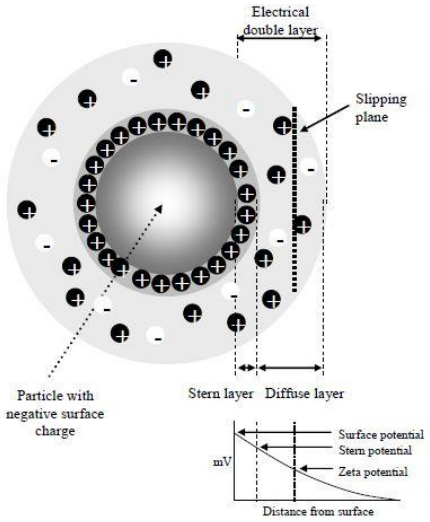

Figure 2-1 Schematic representation of the distribution of ions around a charged particle in solution. [31]

2.3 Parameters affecting the SPP

2.3.1 DNA factor

DNA is negatively charged in aqueous solution due to the phosphate backbone; in aqueous solution, the phosphates will be ionized by releasing the hydrogen ions and the DNA is negatively charged [34, 35]. The negative charge of the DNA can be utilized to control the effective surface charge of nanoparticles by attaching the DNA molecules to the nanoparticle surfaces.

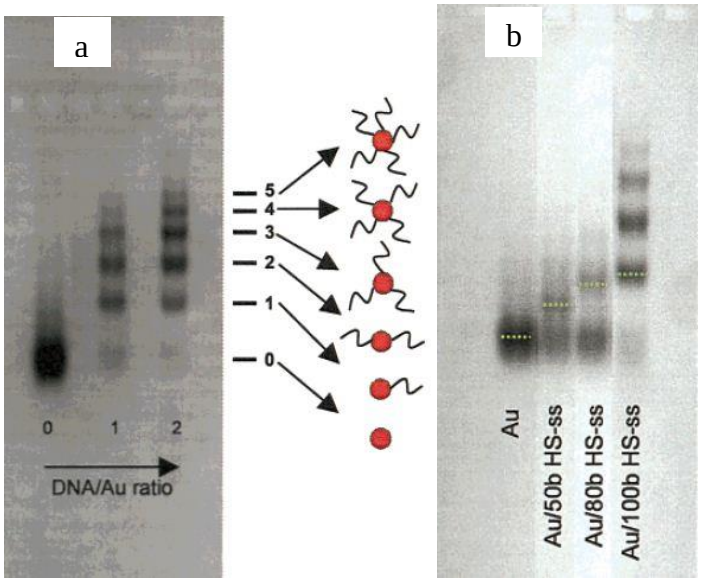

Figure 2-2

(a) Electrophoretic mobility of Au/100b HS-ssDNA mixture with different number of attach DNA bound strands (3%gel) (b) Electrophoretic mobility of single strand Au/HS-ssDNA mixture with different DNA length (3%gel) [36]

Studies demonstrate that particle surface charge can be increased by attaching the DNA to nanoparticles. Daniela Zanchet [36] showed that conjugating 5nm Au nanoparticles with HS-ssDNA increased the nanoparticle surface charge. They used the modified particles to do electrophoretic experiment (gel 3%) and the result shown that the Au/DNA conjugate mobility increased. What is more, the result also shown that the more DNA strand loaded on particle surface, particle mobility increased non-lineally. Figure 2-2(a) shown that the different electrophoretic mobility of binding stand number equal to 0, 1, 2 respectively. The length of loaded DNA strands was another factor affected the particle mobility. Longer DNA chain meant more phosphate on DNA structure, and they will supply more negative charge. Figure 2-2(b) shown that with the length of DNA

strands which attach on Au particle surface increased, the Au/DNA mixture electrophoretic mobility increased.

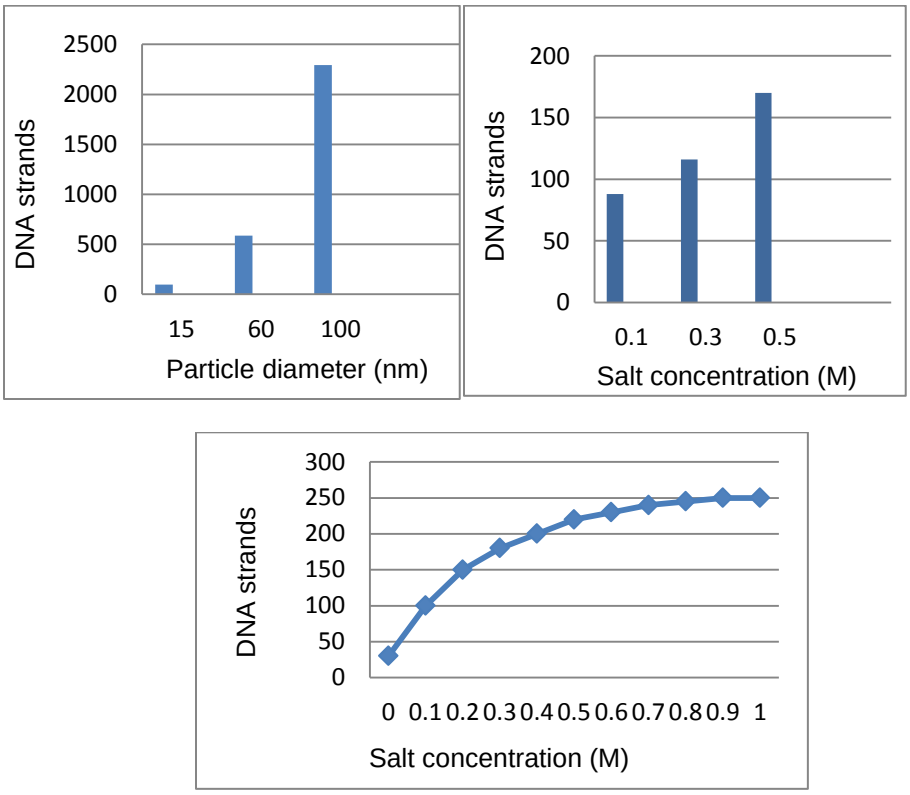

Figure 2-3 (a) Number of DNA strands with different particle diameter (b) Number of DNA strands with different salt concentration (c) Roughly tendency of number DNA strands vs salt concentration

Another thing worth to pay attention is the number of DNA strands load on particle surface can be affect by two factors. According to Angel S. Butron, in his paper "Nano Lett, Vol. 1, No. 1, 2001" [37] mentioned the number of DNA strands load on particle surface determined by particle size and salt concentration. DNA strands increase proportionally as gold particle size increase. He used 15, 60, 100nm gold particles to do experiment and the result clearly shown 96, 586, 2294 DNA strands are load on gold particles respectively (Figure 2-3 (a)). From Figure 2-3 (b) it can see that the DNA

strands load on Au particle surface also increase when salt concentration in solution increase. Without any other parameter change, the average number of DNA strands for 0.1M, 0.3 M, and 0.5 M salt concentration are 88, 116, and 170 respectively. Actually, unlike particle size parameter, the relationship between the number of DNA strands and salt concentration is not linear relationship and when salt concentration arrive some specific point DNA strands will not load on particle anymore. Figure 2-3 (c) exhibits rough tendency of relationship between DNA stands on particle surface and salt concentration.

2.3.2 Ionic concentration factor

The ion concentration also called ion strength can affect the zeta potential of particle. It can image that, if a lot of free ions exist in solution. They make the double layer more condense and decrease the zeta potential dramatically. In opposite, if there are less free ions in solution, particle will form double layer very difficult and the double layer is loose. So, particles can aggregate and form a cluster in the high ion concentration solution but they will separate from each other in the low ion concentration solution [38, 42]. The valence of ion also influences the zeta potential of particle. For example, the double layer which formed by Na^{+} ion (+1) is thinner than that formed by Mg^{2+} ion (+2) [43].

2.3.3 pH factor

Another experiment factor affect the experiment result is buffer pH. Sometime the buffer pH can even change the positive-negative sign of zeta potential it changes a lot. In real case, we combine the ionic concentration and buffer pH to measure the particle zeta potential [43]. The follow picture Figure 2-4 shows the relationship of zeta potential and pH for SiO2 in water with different salt (KNO3) concentration. According to “R.J. Hunter in his paper ‘Zeta Potential in Colloids Science’, *Academic Press*, NY, 1981” [24] shown: if user wants to get high zeta potential, can decrease the buffer pH and increase the salt

concentration. If user needs low zeta potential, we can increase the buffer pH and decrease the salt concentration.

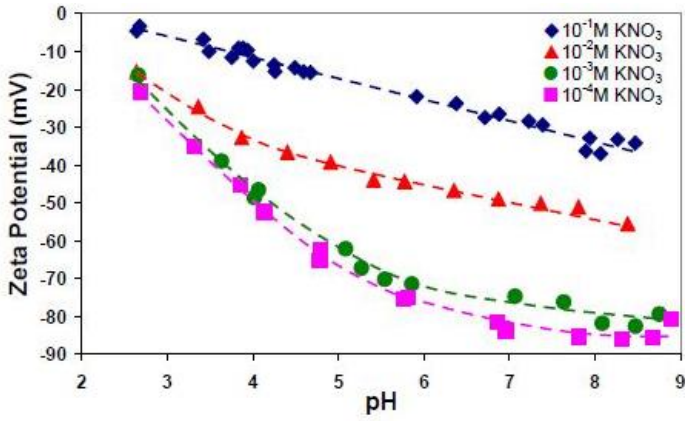

Figure 2-4 pH vs zeta potential of different salt concentration [24]

Except the particle zeta potential, the buffer pH can also affect the SPP process in two ways. First it changes the charge of DNA molecule [44, 45]. It means the charge of DNA-particle conjugation depends on the solution pH. As Chapter 2.3.1 mentioned, DNA appears electronegative due to phosphates on its backbone. The phosphates will release the hydrogen ions. So, at the moment when the alkali adds into the buffer, the hydrogen ion will be neutralized byhydroxyl ion and lead DNA become more negative. Same thing, when adding acid into buffer, the addition hydrogen ions surround particle will tend to attach on DNA surface and neutralize some negative charge of DNA. In this condition, the DNA-particle will decrease its surface charge.

Solution pH can also change the substrate surface charge. It is another way that solution pH affect SPP process.

At beginning, let us display the process of APTES attach on template surface by SAMs. As Figure 2-5 shows [46]. The silicon wafer surface will link the hydroxyl group [-OH] under the alkali environment. When APTES come, the [-OH] on silicon will combine the [-EtO] on the APTES (EtO means in ethanol solution) generate H_2O and ether [-O-],

in this way the APTES is combine with silicon surface. And it is known each APTES have three [-EtO]s, one of them combine the Si surface and other two [-EtO]s will combine with [-EtO] on anther APTES to generate H_2O and ether [-O-].

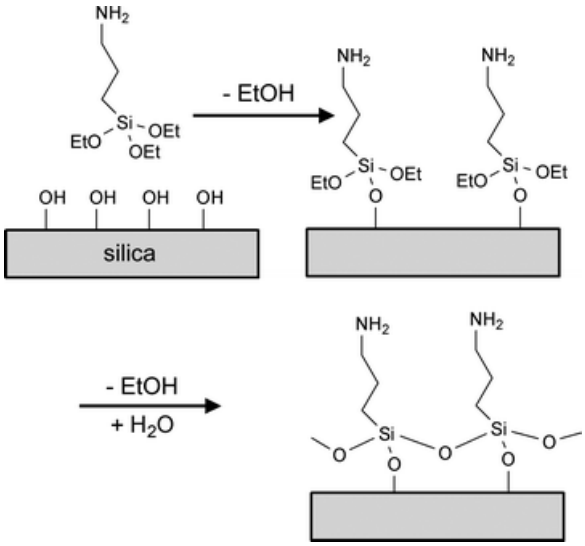

Figure 2-5 Process of APTES link to silicon surface [46]

Next, let us figure out the process of MHA link to gold surface by SAMs [47]. As Figure 2-6 shows. The thiols have strong affinity to noble metal such as gold, so when immerse the gold layer in MHA ethanol solution the group [-SH] can link to the gold surface.

It can notice that the APTES have the function group [$-NH_2$]. In the aqueous solution the [$-NH_2$] group will gain a [H^+] change to [$-NH_3^+$], this is the reason APTES make silicon surface positive charge. Similar, the MHA have the function group [-COOH], in the aqueous solution the [-COOH] will lose a [H+] to become [-COO-], and this is the reason MHA make gold surface negative charge. It can imagine that if the solution pH is very high, which means there are many free hydroxyls [-OH] in solution and they will restrain the [-NH2] to gain [H+] ions, that will lead silicon surface which attach with APTES become less positive charge or even electric neutralize. If the solution pH is very

low, which means there are many free hydrogen ions [H+] in solution and they will restrain the [-COOH] to release [H+] ions and lead the gold surface which attach with MHA become less negative charge or even electric neutralize. So, in this view, it is important to make the PB solution pH at some specific point (for example pH=7) which is low enough for APTES to gain [H+] ions and at same time it is high enough for MHA to lose [H+] ions.

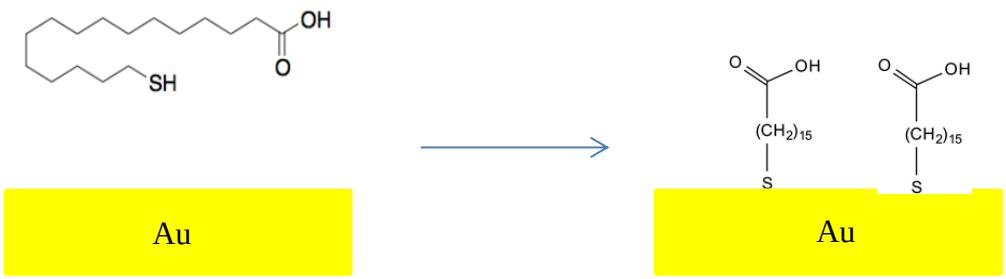

Figure 2-6 Process of MGA link to gold surface

Actually, Fei Huang in his thesis [48] “Sensitive detection of clozapine using a gold electrode modified with 16-mercaptohexadecanoic acid self-assembled monolayer” indicated: the buffer pH can influence the MHA surface electrostatic potential. Figure 2-7 shows when buffer ($0.05 molL^{-1}$) pH increase the MHA layer peak current and peak potential shift obviously. When PB solution pH=7 the MHA layer peak potential around 1.2V, while when PB solution pH=8 the MHA layer peak potential reach the max 1.6V.

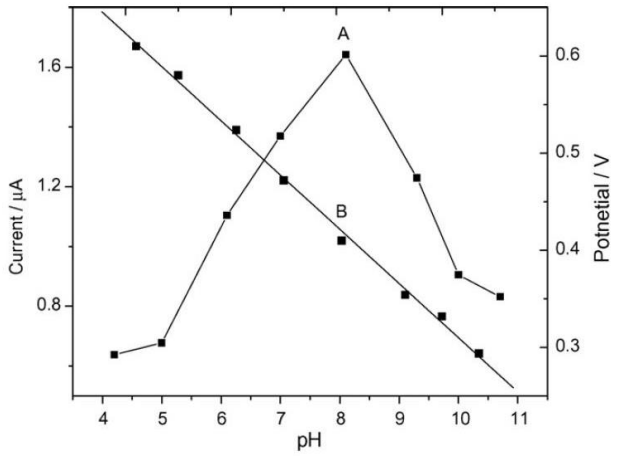

Figure 2-7 MHA surface electrostatic potential (line B) vs buffer pH [48]

Inclusion, there are two thing about buffer pH affect SPP process need to be noticed. One thing is when solution pH increase the DNA-particle surface charge will increase. Another thing is solution pH should maintain at the crucial point which both good for APTES to gain positive charge and MHA to gain negative charge.

2.4 The calculation of Debye Length

This thesis designed several series of circular templates with varying diameter to do SPP experiment. It can roughly design the range of diameter by experience according to data. But it is more academic and accurate to design the circle diameter range by calculating the particle Debye Length [49, 51]. When colloidal particles are dispersed in a medium containing free ions, the electrostatic interactions will be screened by these ions. The net “double-layer” interaction decays roughly exponentially with a characteristic length called the Debye length κ-1. For example if the particle A has charge –Q and its Debye length is λ. If the distance from particle A over than λ can be think as neutralize. In other word, the free ions surround the particle will form a charge sphere which radio equal to λ. This sphere will totally shield the particle charge. Because within the sphere

the total charges from ion are approximately equal to +Q. It can cancel the –Q charge from particle A [52].

The Debye Length calculation can give as equation 2.1:

$$\kappa = [(1000e^2 N_A / \epsilon\epsilon_0\ kT) \sum_i Z_i^2 M_i]^{1/2}$$

Where:

K: Inverse of Debye Length

N_A: Avogadro's number

Z_i: Valence of ion species i

$M_{i:}$ Concentration of ion species i

$\epsilon_{0:}$ Permittivity of free space

ϵ: Dielectric constant of water

This thesis used three different salt concentration solutions (0.1mM, 0.05mM and 0.01mM) as the experiment solution. PB solution contain [Na^+], [PO_4^{3-}], [HPO_4^{2-}], [$H_2PO_4^-$], [H^+] and [OH^-] ions. Here an approximate treatment is given: choose PB solution pH=7 to processing calculating, in this solution because the hydrogen ion concentration equal to the hydroxyl ion concentration ([H^+] = [OH^-]) it means no [H^+] contribute by reactant Disodium phosphate or Monosodium phosphate. So it can approximately think no intermediate product [PO_4^{3-}] and [H_3PO_4] exist, all reactant are complete ionization.

According to calculation, in 0.1mM PB solution pH=7, the Debye Length is 56.5nm; in 0.05mM PB solution pH=7, the Debye Length is 126.3nm; in 0.01mM PB solution, the Debye Length is 178.6nm.

Chapter 3

Experimental design

3.1 Introduction

In this Chapter, experimental procedure is presented. First, this part will introduce the method to make the experimental template. The thesis fabricated two kinds of template, the negative resist template and the positive resist template. Both of them have their own characteristic. Negative resist template made pattern complex but fabrication process was difficult while positive resist template could fabricate easily but pattern shape were simple. Thereby in our experiment, we focused on negative resist template. Then this Chapter demonstrated the method to produce P30 particle (the probe-DNA and 30nm Au particle conjugation) in detail. This part also demonstrated the whole experiment process step by step including how to build the desirable pattern on template surface and how to set up the electrostatic guiding structure.

3.2 Template fabrication

3.2.1 Negative resist template

Because the process to fabricate negative resist template and positive template are similar except a part of reagent and the template pattern shape are different. So this part chooses the negative resist template as an example to introduce fabrication process.

First, using diamond crack to cut Si wafer into appropriate size, around 2cm*2cm. Then immersed the template with acetone and clean by ultrasonic cleaner 10mim. After that, dry the template with nitrogen gas and place the template on the hot plant, we bake the template at 200°C 20min. Table 3-1 shows some raw materials.

Table 3-1 Reagent and materials

Status	Name
Solid	<100> Silicon wafer 475-575um
Liquid	Acetone
Liquid	Methanol
Liquid	Ethanol
Liquid	Developer Ma-D 525
Colloid	Ma-N 2403 photoresist

When the template is totally dry, cover the resist layer on template surface by using Ma-N 2403 negative-photoresist and uniform the layer thickness by using Spin coater: S/N pw3200960-D. Table 3-2 is the parameter of spinning. The photoresist resist is soft and can be easily removed. So heat the template on hot plant at 95°C 3min is necessary to strength the resist layer. The color of resist layer will change during the heat process: from green to yellow and it is convenient to us to know the whether the resist later is soft or firm. This template is ready to process lithography now, making the small mark on resist surface by diamond cracker, and in later the mark can help to assign the pattern location during the lithography.

Table 3-2 Spin coater parameter

Step	Speed	Ramp (rpm)	Time (sec)
1	500	100	5
2	4000	1000	30

The pattern was designed by software Auto-CAD as Figure 3-1 show. The pattern “Au” and “Pt” letter were composed by small holes. In one letter every holes diameter are size. But the diameter is different in different letter. The sizes of holes increase gradually, from the first line 150nm to the last line 300nm. In the top right corner the patterns size also increase from 150nm to 300nm. Several groups of lines with 1um length and different width are placed at the bottom right corner.

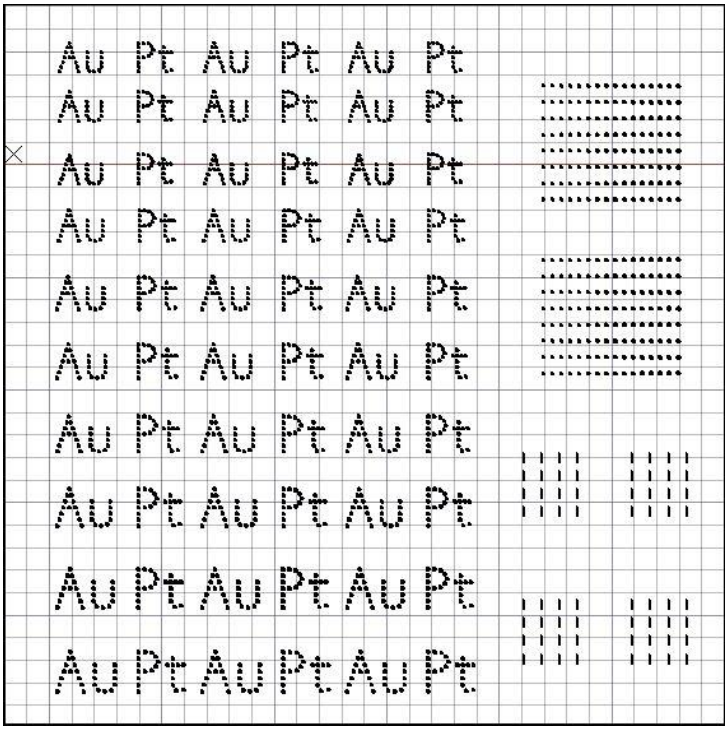

Figure 3-1 Pattern of Auto-CAD

Table 3-4 shows the parameter of photolithography.

During the photolithography process, the resist which are exposed in electron beam will become firm. Then put the template into developer Ma-D 525 60sec and the soft resist which are not exposed in electron beam will be removed [53]. Washing the template in DI water 5min after develop is necessary because there are some resist residual may remain on the surface. Later, dry the template by nitrogen gas.

Table 3-3 Parameter of photolithography (both two kind of template)

Type	Normal writing
Magnification	4500
Center to center distance	2.5 nm
Line spacing	2.5 nm
Aperture	3
Measure beam current	35.0 pA
Dwell color	0.358 usec
Area dose	200 uC/cm^2

Now, the pattern is formed on the template surface. The next step is deposition the gold on the template surface [54, 56]. The deposit device is E-beam evaporator AJA, we deposit Chromium layer 5nm and gold layer 15nm on template (Table 3-4 shows the parameter of e-beam evaporator). The chromium functions as medium binder between gold and silicon

Table 3-4 Parameter of evaporator (both two kind of template)

	Cr	Au
Rate (A/sec)	1.1-1.5	1.1-1.5
Thickness (nm)	5	15
Emission current (Kv)	25-28	28-30
Density (gm/cm^2)	7.2	19.3
Impedance	28.95	23.18

As Figure 3-2 show, the gold layer attach on silicon template is stable however the resist which cover on the resist are unstable since the resist are easily clean up by acetone. So the pattern can form by immersing the template in acetone 30 min. Finally clean the template with acetone 10min plus ultraviolet-light cleaner 20min, 5 circles.

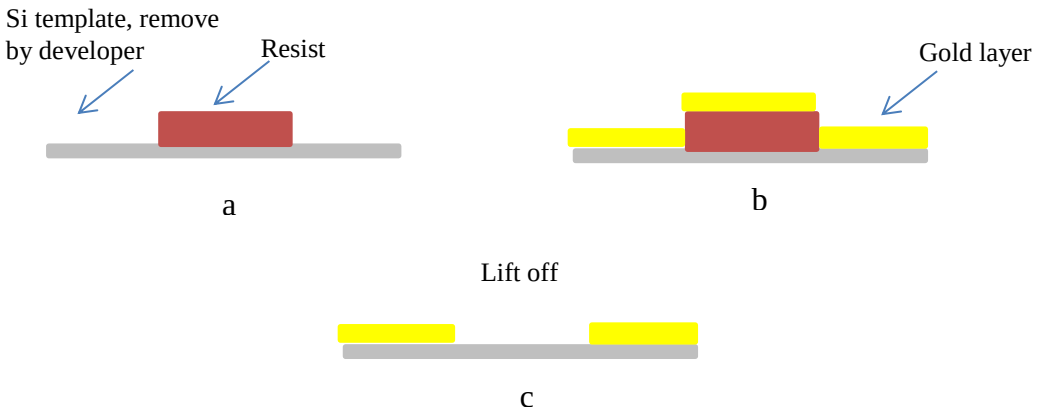

Figure 3-2 (a) After develop the firm resist remain on the silicon template surface (b) Deposit the gold layer on the template (c) Lift off by acetone, the gold layer cover on resist is gone

3.2.2 Positive resist basic template

The main idea of positive resist basic template is almost same as the negative resist basic sample. Except the pattern shape and some reagent are different.

At beginning, clean the silicon template with acetone 10min and UV-cleaner 20min. Then coat the positive resist PMMA A4 950 on the template surface. Follow is the reagents and materials (Table 3-5):

Table 3-5 Reagent and materials

Status	Name
Solid	<100> Silicon wafer 475-575um
Liquid	Acetone
Liquid	Methanol
Liquid	Ethanol
Liquid	Developer 2-propanol and 4-methyl-2-pentanone mixture
Colloid	PMMA A4 950

The parameters of spin coater as Table 3-6 shows:

Table 3-6 Spin coater parameter (positive resist)

Step	Speed(rpm)	Ramp(rpm)	Time (sec)
1	500	100	5
2	4000	1000	40

Prepare-baking at 185°C 2min is necessary to firm the resist layer. After at do the photolithograph, the pattern is design with Auto-CAD see the Figure 3-3. The blue area between white hexagons are exposed on electron current, and the line width decrease gradually from right 200nm to left 100nm. In other world, the diameter size of white hexagons area increase gradually. The photolithograph parameter refers the negative resist basic template (Table 3-3). After that, immerse template in positive resist developer MIBK 65sec (which contain 4-Mrthyl-2-pentanone and 2-propanol the ratio is 3:1) to remove the soft resist area [57]. The metal deposit and cleaning procedure are the same as negative resist basic template can refer the chapter 3.2.1.

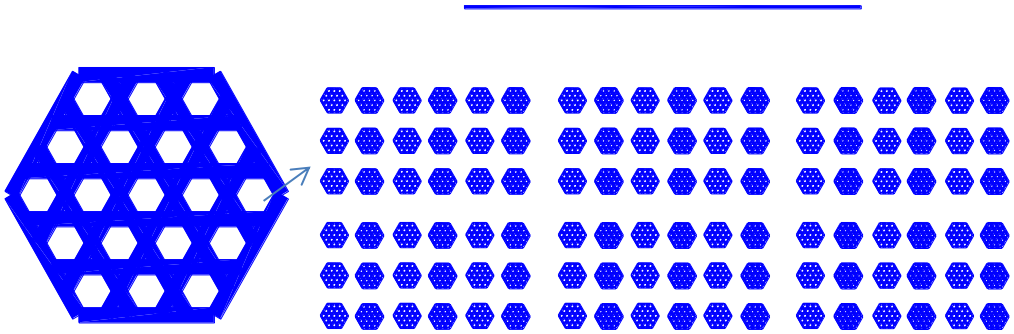

Figure 3-3 Pattern of Auto-CAD

During the lithography process, the area which are exposed by electron current will become soft than other areas and can be easily remove when template is immersed in positive resist developer. Figure 3-4 show the concept of development process. Finally clean the template with acetone 10min plus ultraviolet-light cleaner 20min, 5 circles.

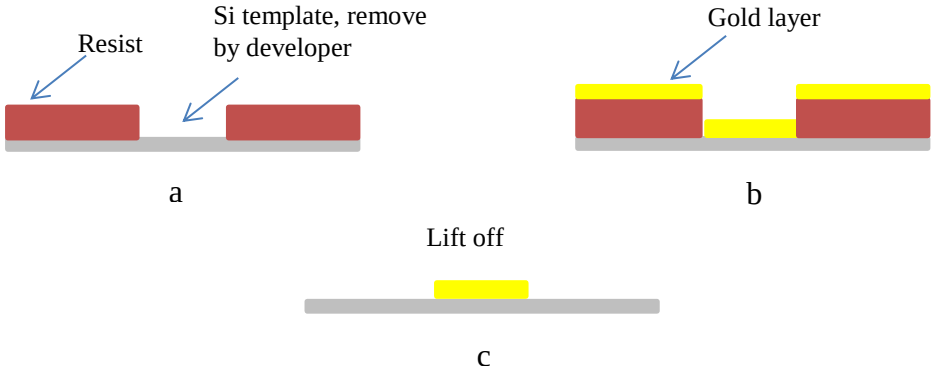

Figure 3-4 (a) After develop the film resist remain on the silicon template surface (b) Deposit the gold layer on the template (c) Lift off by acetone, the gold layer cover on resist is gone

3.3 Electrostatic gating set up

Setting opposite charge on template surface needs two steps of self-assembled monolayers (SAMs). First, immerse the template in 3-aminopropyl triethoxysilane

(APTES) solution which including ethanol 1000ul, 0.1N NaOH solution 4ul, and APTES 5ul for 40min. After this process, the silicon surface will bond with amine group (NH_3^+) which are positive charged. Then clean the template to make sure there is no APTES residual solution survives on its surface. After that, immerse the template in 16-mercaptohexadecanoic acid (MHA) solution which including ethanol 800ul, MHA powder 2.5mg and 37% hydrochloric acid (HCl solution) 8ul for 3hours. The MHA solution can supply carboxylate group (COO^-) on gold surface to make gold surface negative charged. Cleaning the template when immersing process is finished, make sure no MHA residual remain on template surface. As far now, the positive charge are functioned on gold surface and negative charge are functioned on silicon surface and placing the negative nanoparticle in template become possible (Figure 3-5 shows the simulate diagram).

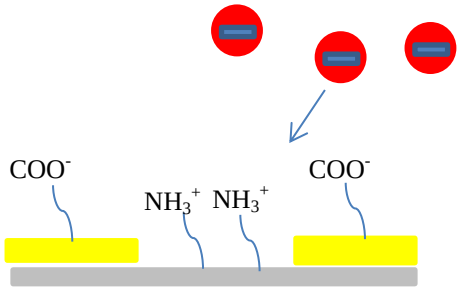

Figure 3-5 Electrostatic gating

3.4 Preparation of experimental particle

This thesis uses 2 kinds of element nanoparticle as experiment particle. One is 30nm platinum particle and other is 30nm gold particle. Use the original pure Pt particle without any special treatment while we conjugate the gold particle with DNA to fabricate the P30. These experimental nanoparticles are order from nanoComposix industry. Figure 3-10 is the picture of raw materials.

At beginning this Chapter will introduce the procedure to make P30. The Table 3-7 is the materials for making P30:

Table 3-7 Materials for making P30

Status	Name
Colloid	30 nm gold nanoparticle
Powder	10D probe-DNA (P-DNA)
Powder	DL-Dithiothreitol (DTT)
Solid	NAP^{TM}-5 column
Status	Name
Solution	Phosphate buffer
Solution	Zonyl-FSN-100
Solution	5M NaCl 10XPBS
Solution	5M NaCl 10mM phosphate buffer
Solution	Tris-EDTA buffer (TE)

First, centrifuge the P-DNA in centrifuge machine at speed of 3000rpm for 3min to make sure the DNA powder sank to the tube bottom and prevent DNA powder from blowing away when user open the tube lid.

Second, cleave the P-DNA. The DNA chains at beginning are linked together and form very long chain. We use 0.1M DTT in 0.2M PB solution 125uL to break the chain at the sequence (-SH-) [58]. After that the DNA chains become shorter and specific purine sequence (-SH) which is used to link the Au particle surface is exposed on its tip. Then shake the tube 3 hours.

Third, elute DNA by NAP-5 column. After cleave DNA by DTT, the tube can contain DNA with specific purine sequence (-SH) which are need, DNA without specific purine sequence, free “SH” purine and DTT solution. So we need to filter away the impurity and only let the DNA which contain “-SH” purine sequence remain. The method is:

a) Put the NAP-5 column in the room temperature wait for use.
b) Open the lip of column and allow the storage solution in column flow away by gravity.
c) Inject the PB solution 12mL into the column. Allow the PB solution enter the gel bed and flow away by gravity.
d) Load the broken DNA 125uL into the column and allow the solution enter the gel bed and flow away by gravity.
e) Inject PB solution 375uL into the column and allow the solution enter the gel bed and flow away by gravity.
f) Elute the DNA by using PB solution 0.5ml.

(Note: the PB mention above are all 10mM PB solution pH=7.5)

Fourth, Stabilize gold particle via coat with non-ionic fluorosurfactant Zonyl-FSN-100 and load the P-DNA onto gold particle surface [59, 60]. Add sodium chloride into solution before loading the P-DNA. The gold particle can aggregate in high salt concentration, so we add the Zonyl-FSN first to coat the gold particle and prevent them from aggregation. The method is:

a) Diluting the Zonyl-FSN-100 solution into 1% concentration.
b) Mix the gold particle 950ul with 1% Zonyl-FSN-100 50ul. Shake the mixture for 15min.
c) Mix purified P-DNA 125ul with 1mL stabilized 30nm gold particle.
d) Add 111uL of 5M NaCl 10XPBS and 14uL of 5M NaCl 10mM PB solution pH=7.5 into the mixture and shake them for 1 day.

Fifth, Purify the P30 by centrifuge machine. After load the P-DNA to gold particle, the mixture contains P30 which we need, free DNA chain, free gold particle and salt solution, so we need pure the mixture and only let the P30 remain. Centrifuge the mixture at the

speed of 10000rpm for 10min. Remove the supernatant and re-suspend 10mL 0.1M NaCl in10mM PB solution pH=7.5. Repeat this process 4times and the last time add the TE buffer instead [61].

Finally, store the pure P30 at 4°C in refrigerator.

As Chapter 2.3.1mentioned, the salt concentration can affect the number of DNA strands link to gold particle surface. Higher salt concentration means more DNA strands attach to gold particle. But if the salt concentration is too high, in experiment the P30 will difficult enter into the pattern because too much negative charge on P30. What is more, the P30 might aggregate when the salt concentration is high enough. In other condition, if the salt concentration is too low. It may not have any difference between P30 particle and the pure gold nanoparticle. So this thesis chooses the salt concentration for making P30 as 0.5M. The salt resources are come from 5M NaCl 10XPBS solution and 5M NaCl 10mM PB solution. P30 salt concentration as follow calculation shows:

$$\frac{950 * 0 + 50 * 0 + 125 * 0 + 111 * 5 + 14 * 5}{950 + 50 + 125 + 111 + 15} = 0.5M$$

At this salt concentration, nearly several hundred of probe DNA attach to the gold surface.

The PB buffer strength can calculate as follow:

$$\frac{950 * 0 + 50 * 0 + 125 * 10 + 111 * 100 + 14 * 10}{950 + 50 + 125 + 111 + 14} = 10mM$$

Chapter 4

Experimental result and analysis

4.1 Introduction

In this chapter, the whole procedure of experiment will be presented. Then a mathematical analysis and discussion about the experiment data will be given.

This thesis is focused on negative resist basic template, so the main assay data is about negative resist basic sample. It show the experiment data in the order as (1) Salt concentration parameter (show the experimental data of P30 in PB solution with different salt concentration). (2) pH parameter (show the experimental data of P30 in PB solution with different pH). (3) DNA parameter (compare the pure platinum particle in PB solution and P30 in PB solution). (4) some data of positive resist basic template(compare the placement condition of particle between two different resist basic samples in same PB solution).

4.2 P30 particle in PB solution

In chapter 2.3 it mentioned that the solution pH and ion concentration can influent the particle's zeta potential and electrostatic force between particle and template surface by referring the theory. As for our experiment the solution pH and ion concentration change can lead to different particle attachment on template surface.

4.2.1 PB solution with different ionic concentration

Ion concentration can be the main factor for particle double layer thickness. High concentration means the particle have more chance to absorb ions which are opposite charge in solution. In high ion concentration solution, the particle's double layer becomes more condense and the total charges of particle will decrease prominently due to the more ions cover the particle surface and these ions will neutralize the particle charge.

Low ion concentration means particle can hardly “meet” opposite charge ions in solution, and will have much less chance to decrease its zeta potential. In another word, low ion concentration can keep particle remain high repulsive force in solution. The limitation of low concentration is zero ion concentration and it called DI water and it is acceptable for experiment. However the high ion concentration also has its limitation because when we increase the ion concentration the particle zeta potential decrease, when zeta potential achieve at some critical point the particle will aggregate. Their repulsive force cannot great enough to keep they separate to each other. In this condition, we cannot get the accurate experiment data.

The experiment the thesis choose 0.1mM PB solution 0.05mM PB solution and 0.01mM PB solution pH=7 as experimental solution. Here the 0.1mM 0.05mM and 0.01mM are buffer strength, the ion concentration are close to 1mM 0.5mM and 0.1mM. The viscosities of solution are same and the experimental temperature is around 25°C.

First, the thesis will display the particle attachment condition in blank silicon wafer, because only the particle attachment condition is saturate can prove the template surface is clean enough and the data is reliable. Figure 4-1 (a) shows the P30 in 0.1mM PB solution pH=7 Figure 4-1(b) shows the P30 in 0.05mM PB solution and Figure 4-1 (c) shows the P30 in 0.01mM PB solution pH=7. From the figures it can see the particle placement condition from these data are all saturate, particles attach to template surface perfectly means we can trust the other data in these three samples. Another important thing is it can see the ion concentration parameter affects the particle placement roughly though these figures. In Figure 4-1 (a) which is 5 times high ion concentration than Figure 4-1 (b) and 10 times than Figure 4-1(c), so particle’s repulsive force is low and can reflect to the distance among the particles.

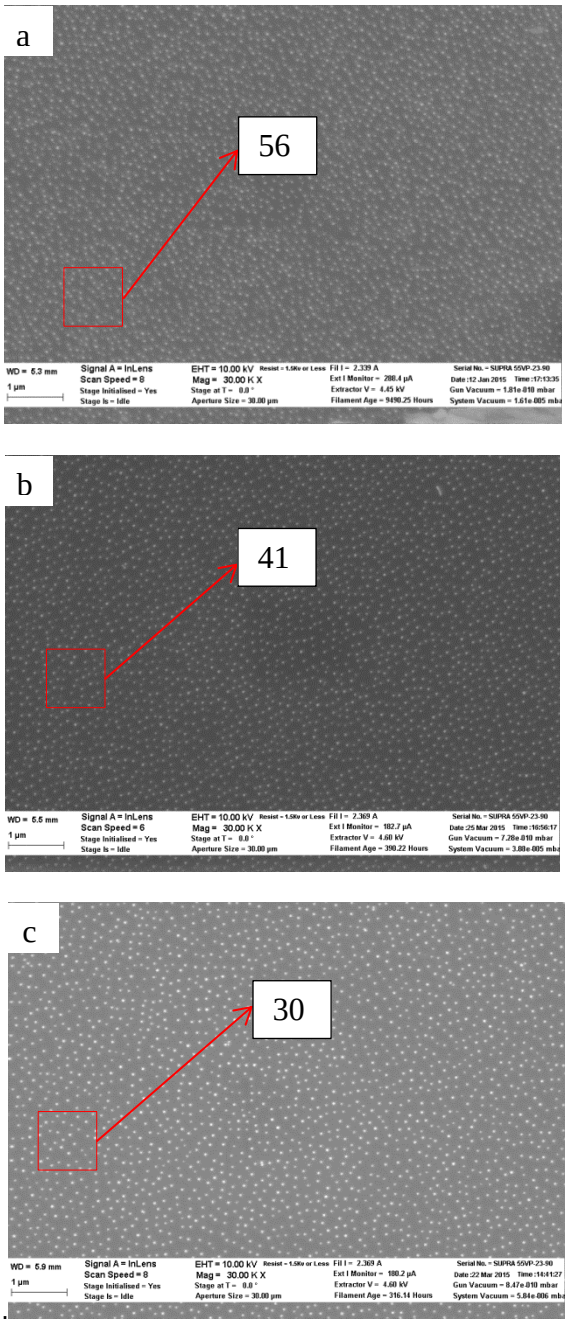

Figure 4-1 P30 attachment condition in blank Si wafer surface (a) In 0.1mM PB solution pH=7. (b) In 0.05mM PB solution pH=7 (c) In 0.01mM PB solution pH=7

By using the SEM can observe the particle attachment on template surface. The magnification of these two figures is 30KX. The red frames in figure are $1um^2$ square and can use to count the particle density of sample. Around 56 particles in the square of Figure 4-1 (a), and the density is $56/um^2$. Same thing, the density of Figure 4-1 (b) is $41/um^2$. It is means when the ion concentration increases 5 times, the attached particle density increase nearly 1.4 times in 2-D area. The distance between particles decreases around 0.85 times. Also, compare with Figure 4-1(b) and (c) the attached particle density increase 1.4 times in 2-D area. The distance between particles decreases 0.85 times.

The Figure 4-2 shows the P30 particle placement condition in different size of holes. The solution are 0.1mM PB pH=7, 0.05mM PB pH=7 and 0.01mM PB pH=7. Several series of holes were designed in software Auto CAD, their diameter from 160nm to 300nm (in real case their diameter will increase a little). With these holes we can measure the repulsive force of particle. For example, when the particle can enter into the holes with 250nm diameter but cannot enter into the holes with 200nm diameter. Its zeta potential is higher than the particle which can enter into the 200nm diameter holes. From Figure 4-2(a) we can find the particle placement is good even in the smallest size holes. The whole template is filled with P30 particles.

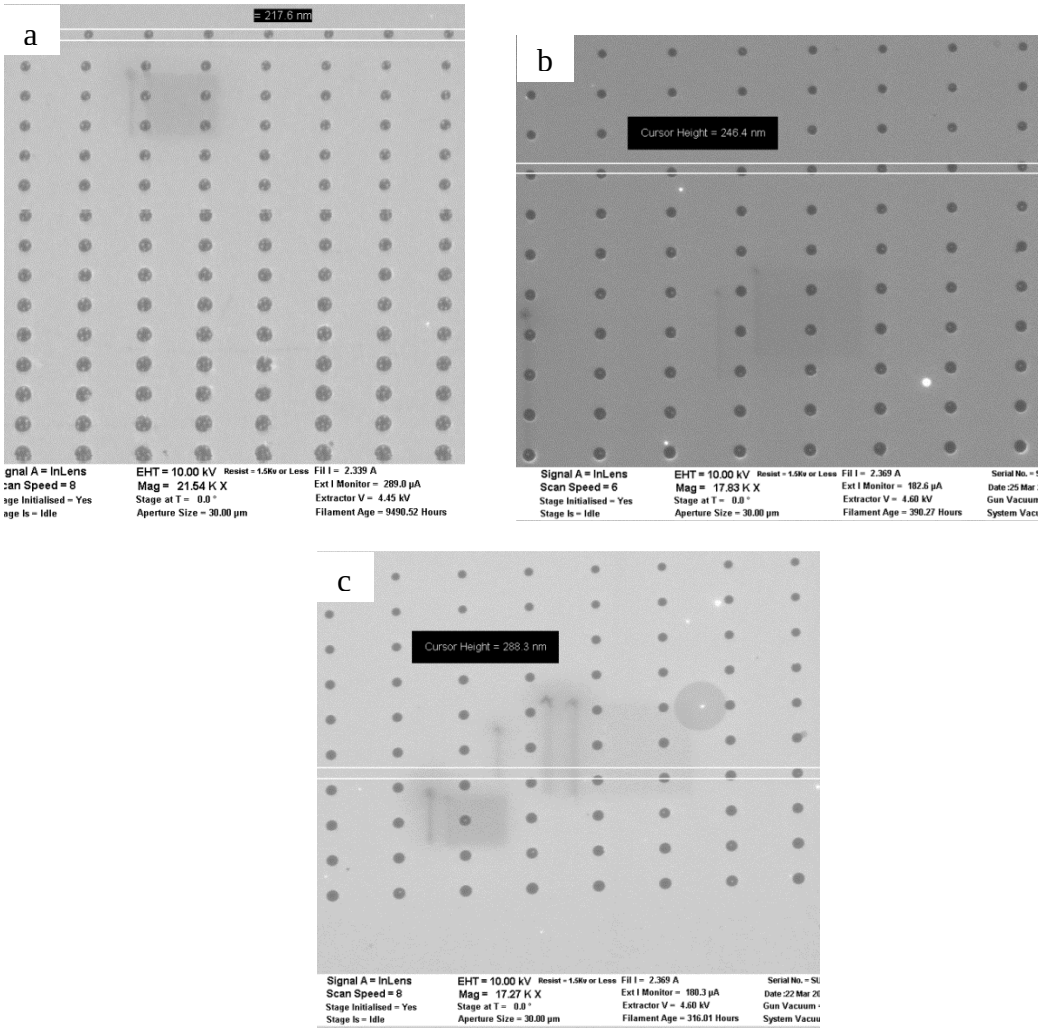

Figure 4-2 (a) P30 in 0.1mM PB solution pH=7 (b) P30 in 0.05mM PB solution pH=7 (c) P30 in 0.01mM PB solution pH=7

The pattern have 8 groups of hole pattern, each group have 16 holes with different diameter from 150nm to 300nm. In real case the holes' size will increase a little. Let us call them from "hole 1" to "hole 16" respectively and make the line chart to reflect average number of particles in each hole. For example, "hole 1" stand for the hole with 150nm diameter and we have 8 "hole 1". If 5 "hole 1" contain 1 particle, and 3 " hole 1" contain 0 particle, the average particle number of "hole 1" is (5*1+3*0)/8=0.625≈0.6. And

It combine the line chart of 0.1mM PB solution 0.05mM PB solution and 0.01mM PB solution together to compare the difference.

From Figure 4-3, know if user need only one particle enter each hole (the idea case), we can choose 0.05mM PB solution pH=7 with hole size equal to 250nm, 260nm or 270nm. It also can choose 0.1mM PB solution pH=7, but we need to decrease the holes' minimum diameter at 100nm.

Table 4-1 Average number of particles in hole with different ion concentration

	0.1mM PB solution	0.05mM PB solution	0.01mM PB solution
Hole 1	1.8	0	0
Hole 2	2	0	0
Hole 3	2	0.1	0
Hole 4	2.4	0	0
Hole 5	2.5	0.1	0
Hole 6	2.5	0.3	0
Hole 7	2.5	0.4	0
Hole 8	3.3	0.4	0
Hole 9	3.6	0.5	0
Hole 10	4.4	0.6	0
Hole 11	4.5	0.9	0
Hole 12	4.3	0.9	0
Hole 13	4.6	0.8	0.1
Hole 14	5.2	1	0.3
Hole 15	5	1	0.3
Hole 16	5	0.6	0.3

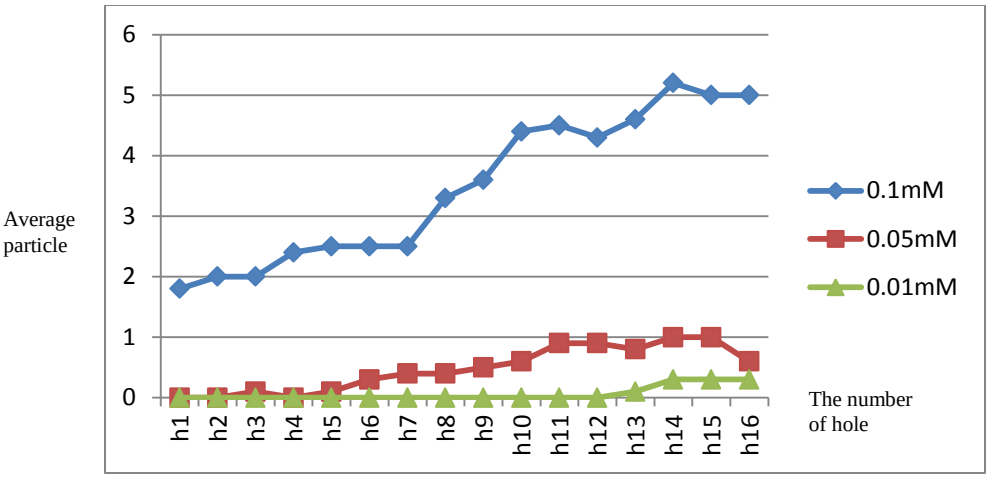

Figure 4-3 Average particle number in each hole with different ion concentration

Next, combine the result of P30 particle attachment in “Au” and “Pt” pattern with different ion strength, 0.1mM PB solution 0.05mM PB solution and 0.01mM PB solution. In future, we will place the P30 particles and Pt particle in “Au” pattern respectively. So check the placement condition in “Au” and “Pt” pattern can be necessary. Figure 4-4 (a) and (b) are P30 particle placement condition in 0.1mM PB solution (c) and (d) are P30 particle placement condition in 0.05mM PB solution (e) is P30 in 0.01mM PB solution placement condition respectively. From the Figure 4-4, we can expect: if user want to select different kinds of particle. We can use low ion concentration like 0.05mM PB solution pH=7 and control the holes’ diameter under 200nm. In this case, P30 particles are hardly entering into holes while platinum particles can enter the holes due to they have less negative charge.

This part can conclude, when given the solution with all parameters like pH, temperature, viscosity and so are same expect the ion concentration are different. The higher ion concentration can get closer placement and the particle are much easier to enter into the holes.

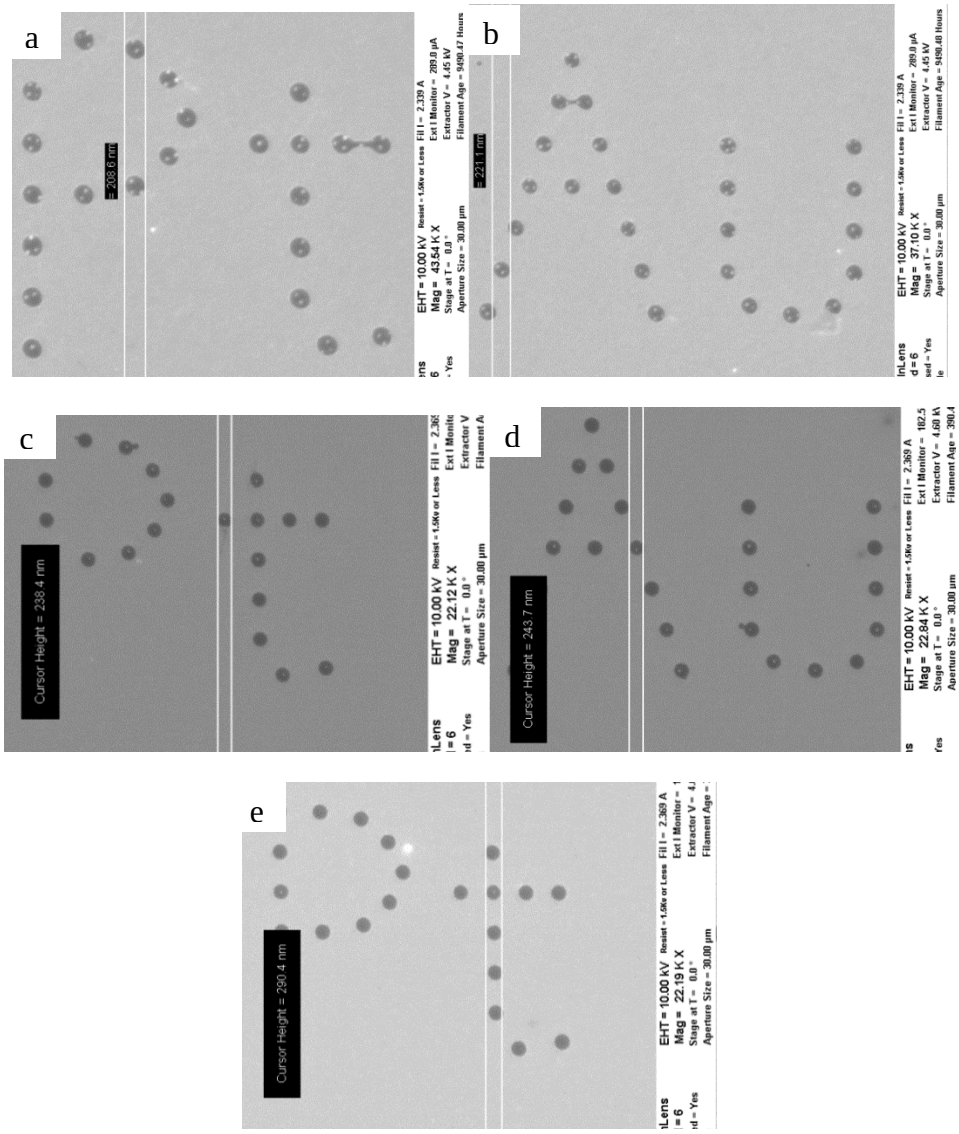

Figure 4-4 (a) P30 attachment condition in “Pt” pattern with 0.1mM PB solution pH=7 (b) P30 attachment condition in “Au” pattern with 0.1mM PB solution pH=7 (c) P30 attachment condition in “Au” pattern with 0.05mM PB solution pH=7 (d) P30 attachment condition in “Au” pattern with 0.05mM PB solution pH=7 (e) P30 particle attachment condition in “Pt” pattern

4.2.2 PB solution with different pH

In the assays, choose solution pH as another controllable parameter for particle placement. As mentioned in Chapter 2.3.3, solution pH can also determine the particles zeta potential. When immerse DNA in low pH solution, the $[H^+]$ ion which come from DNA hydrolysis will be suppressive because the $[H^+]$ ion concentration too high. So, more $[H^+]$ ions which are positive charge attach to DNA and neutralize the whole particle's charge. The particle's zeta potential increase leads to particle placement more easily. In opposite way, when immerse DNA into high pH solution, the $[H^+]$ ions will react with $[OH^-]$ ions in solution and generate H_2O. This process can excite DNA release more $[H^+]$ ions and the rest of DNA charge decrease further. However, it is a reasonable pH range of solution. If the pH too high or too low, the DNA could not survive in the solution, what's more if the solution pH too low, abundant of $[H^+]$ ions attach on particle and sometime even make the particle's zeta potential change to positive. The idea case is solution pH from 6 to 9. In our assay we choose three group of pH as experimental parameter. They are pH=7, pH=7.5 and pH=8. We use monosodium phosphate solid (NaH_2PO_4) , disodium phosphate solid (Na_2HPO_4) and DI water as raw materials, add NaH_2PO_4 and Na_2HPO_4 solid with some ratio in 100mL water to get PB solution with specific pH. The follow table 4-2 shows us the quantity of Na_2HPO_4 and NaH_2PO_4 solid in DI water for each pH. This thesis use 10mM PB as start point, then it can dilute with DI water to get the low concentration buffer. The solution pH can decease a little when dilute the solution.

Table 4-2 Quantity of phosphate in DI water

	Na_2HPO_4(g/L)	NaH_2PO_4 (g/L)
PH=7	1.5	0.6
PH=7.5	2.2	0.3
PH=8	2.5	0.1

In the assay, use 0.05mM PB buffer with pH=7 pH=7.5 and pH=8 as the experimental solution for particle placement. The viscosities of solution are same and experimental temperature around 25°C.

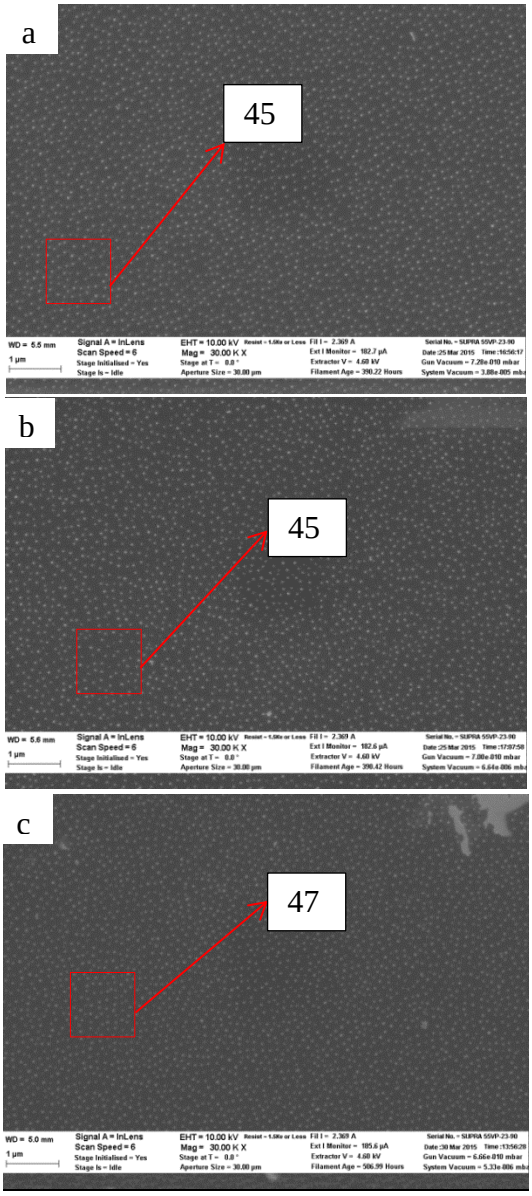

Figure 4-5 P30 attachment condition in blank Si wafer surface (a) In 0.05mM PB solution pH=7 (b) In 0.05mM PB solution pH=7.5 (c) In 0.01mM PB solution pH=8

First, display the attachment condition of P30 particle placement. Figure 4-5 (a) shows the 0.05mM PB solution with pH=7, Figure 4-5 (b) shows the 0.05mM PB solution with pH=7.5 and (c) shows the 0.05mM PB solution with pH=8. From these pictures, it can see the particle attachment on template surface is saturated, which means they are no containment on template surface and the data of these template are reliable, otherwise the P30 particle on template will become cluster and unsaturated.

By using SEM observe the template surface. The magnification of these two figures is 30000X. This thesis used the 1um*1um red square to measure the P30 particle density roughly. In Figure 4-6 (a) the P30 particle in square are 45, the density is 45/um^2, compare with Figure 4-5(b) 45/um^2 and Figure 4-5(c) 47/um^2, there are no much difference. So it can be considered that the main factor affect the particle's zeta potential is ion concentration. Solution pH is the subprime factor of particle placement.

Then give the data of P30 particle placement in pattern, also it can compare with solution pH factor, as Figure 4-6(a) shows the 0.05mM PB solution pH=7 placement condition. Here we just display a part of the pattern. From the picture it can see the P30 particle can enter into the hole when D (diameter of hole) equal to 246nm or even small than this number. The particle placement condition also satisfied the rule which is the bigger hole can contain the more particles. Figure 4-6(b) and (c) display the P30 particle place with the pattern in 0.05mM PB solution pH=7.5 and 0.05mM PB solution pH=8 respectively. Compare with Figure 4-6(a), when pH=7.5 the P30 particle placement condition is similar. The difference is not obviously. But when pH=8, the P30 particle attachment become much less, only when D=320nm the P30 particle begin to enter the holes.

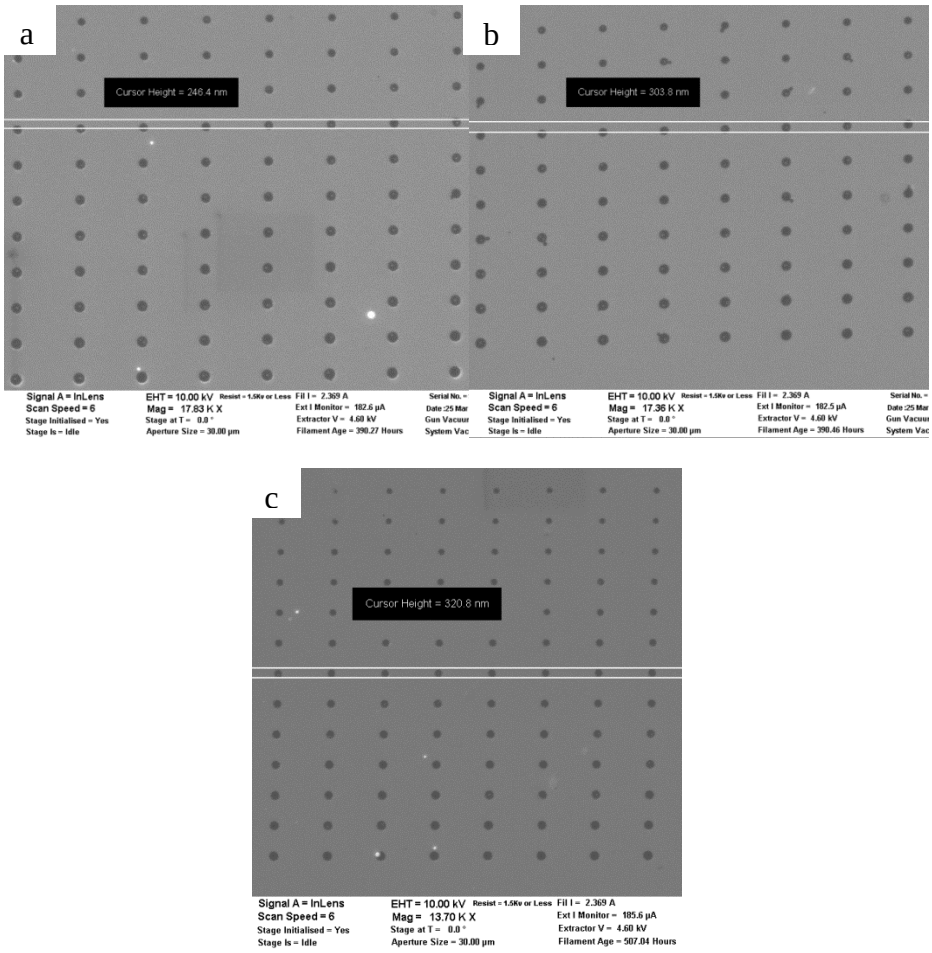

Figure 4-6 (a) P30 particle attachment condition with pattern in 0.05mM PB solution pH=7 (b) P30 particle attachment condition with pattern in 0.05mM PB solution pH=7.5 (c) P30 particle attachment condition with pattern in 0.05mM PB solution pH=8

Here, make the line chart to reflect the placement condition of P30 in 0.01mM PB pH=7 and 0.01mM PB pH=8 visualized. Table 4-3 give the number of P30 particle in each size of hole and Figure 4-8 reflect the change as the holes size increase gradually. Same as Table 4-1, “h1” to “h16” stand for holes’ size from D=150nm to D=300 respectively the real diameter in pattern will increase a little. The result of P30 particle placement condition with pattern shows as the solution pH increase, particle become

more difficult to attach into the hole. The green line which stand for 0.05mM PB solution pH=8 are much lower than blue line which stand for 0.05mM PB solution pH=7 or red line which stand for 0.05mM PB solution pH=8. It is seem the P30 particle suffer higher repulsive force in high pH solution.

From the Figure 4-7, we also notice that the particle attachment in last line (hole 16) trend to decrease while the hole size actually is increase. We think the reason is edge effect. Beside the hole one side in last line are totally gold surface which will provide repulsive electrostatic force on particle, so the particle near the last line could be suffered higher repulsive force that particle near the middle of pattern. That is why particle attachment in pattern's last line decreases.

Table 4-3 Average number of particles in hole with different solution pH

	PH=7	PH=7.5	PH=8
Hole 1	0	0	0
Hole 2	0	0	0
Hole 3	0.1	0	0
Hole 4	0	0	0
Hole 5	0.1	0.1	0
Hole 6	0.3	0.4	0.1
Hole 7	0.4	0.1	0
Hole 8	0.4	0.3	0
Hole 9	0.5	0.4	0
Hole 10	0.6	0.5	0.3
Hole 11	0.9	0.6	0.3
Hole 12	0.9	0.3	0.4
Hole 13	0.8	0.9	0.1
Hole 14	1	0.8	0.3
Hole 15	1	0.9	0.3
Hole 16	0.6	0.6	0

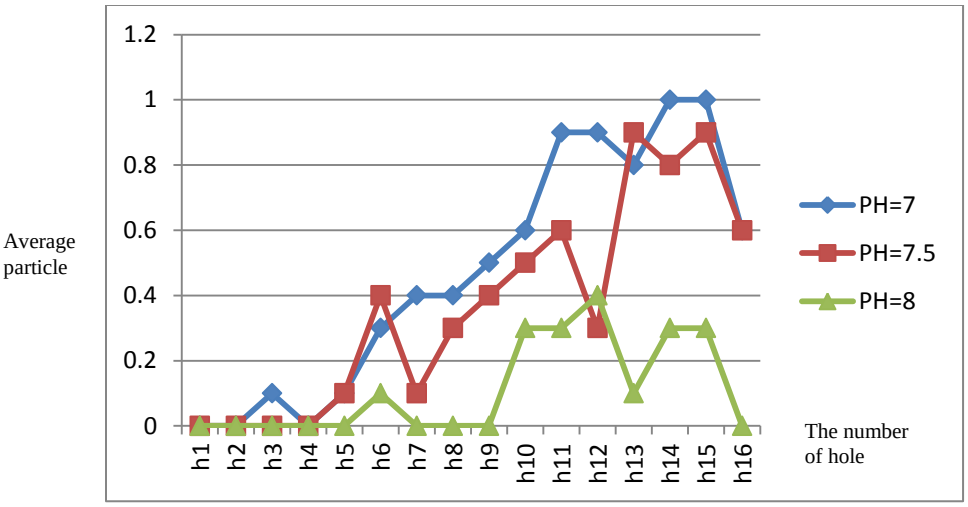

Figure 4-7 The number of average particles in each hole with solution pH

Also from the Figure 4-6 we find P30 particle placement condition in blank silicon wafer appear not much different when solution pH change from 7 to 8. It is seems that the zeta potential of P30 have not changed. So, it deduce the reason that particle become difficult to enter into the hole is because solution pH changes the gold surface electrostatic potential. Gold surface provided higher repulsive force on particle when buffer solution increase. And the buffer pH change the DNA negative charge is minor factor. That is why P30 particle have the same attachment density in blank silicon wafer as pH change from 7 to 8, but still appear the different electrostatic force when P30 attached in pattern. Refer the Chapter 2.3.3, gold surface link to MHA which contain the function group [-COOH]. There is ionic balance formula in water: (equation 4-1)

$$COOH \overset{water}{\Longleftrightarrow} COO^- + H^+$$

Equation 4-1

So, when solution pH increases the [H+] can be consumed quickly with [OH-] to generate H2O. In this way, it will promote more [-COOH] to decompose to [$-COO^-$] and [H^+]. The gold surface electrostatic potential decrease as it contains more [$-COO^-$] instead

of [-COOH]. So, although the charge of P30 particle does not change a lot, the repulsive force between P30 and gold surface increase.

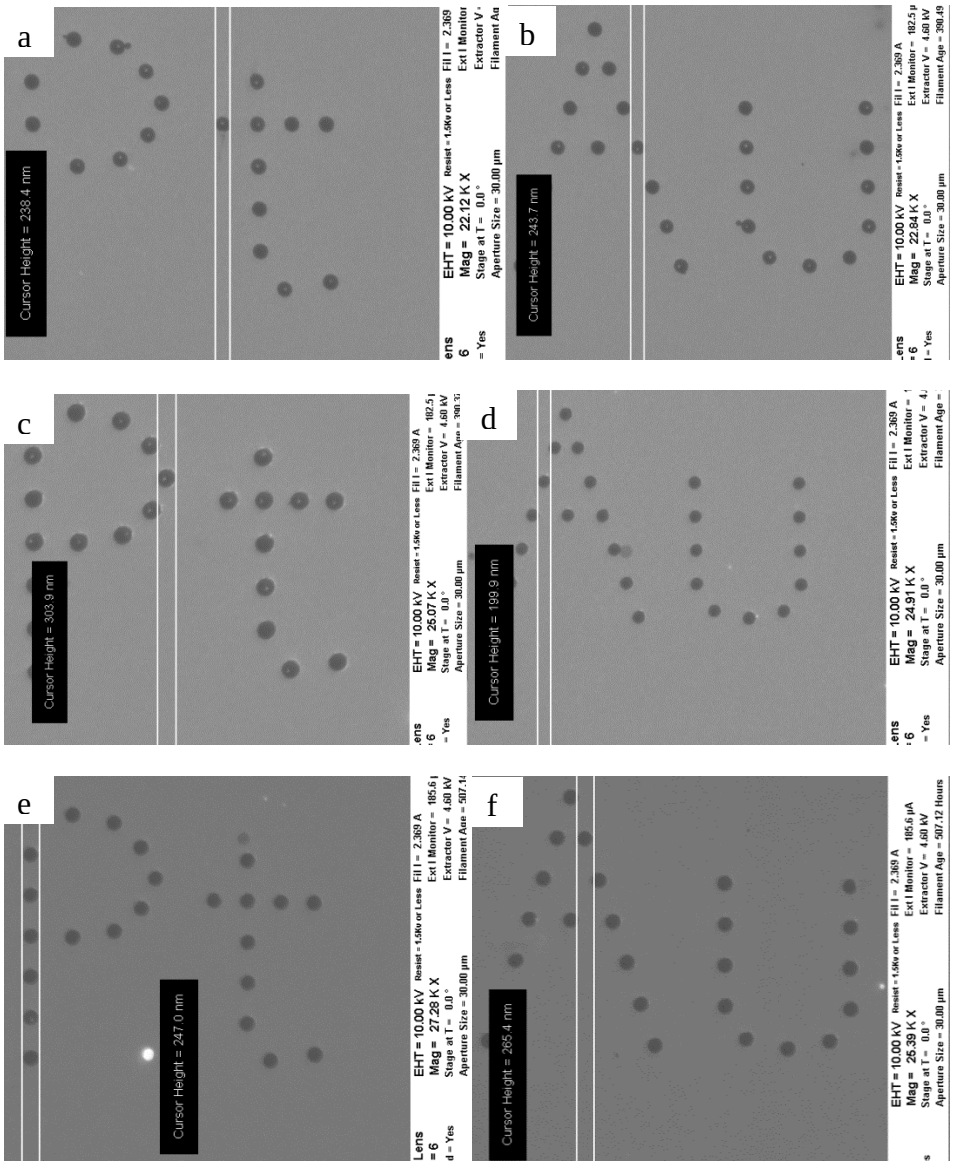

Figure 4-8 (a) and (b) P30 attachment condition in “Pt” and “Au” pattern with 0.05mM PB solution pH=7 (c) and (d) P30 attachment condition in “Pt” and “Au” pattern with 0.05mM PB solution pH=7.5 (e) and (f) P30 attachment condition in “Pt” and “ Au” pattern with 0.05mM PB solution pH=8

Next, show the P30 particle placement condition in “Au” and “Pt” pattern, Figure 4-8 (a) and (b) are for 0.05mM PB solution pH=7, (c) and (d) for 0.05mM PB solution pH=7.5, (e) and (f) for 0.05mM PB solution pH=8. From the 6 pictures can know the P30 placement conditions are similar when pH=7 and pH=7.5, all of them are nearly filled all the holes. While the Figure 4-8 (e) and (f) 0.05mM PB solution pH=8 the P30 particle attachment condition are much less. Only a few of P30 particle filled the holes. Under this way, it can know the P30 particle in 0.05 PB solution pH=7 and pH=7.5 have better attachment than 0.05 PB solution pH=8 in “Au”, “Pt” pattern.

It proves that high solution pH can increase the repulsive force between particle and gold surface. Sometime if user need change the particle attachment density without change the particle self-charge can use this way alter the pH of solution.

4.3 Pure platinum particle in DI water

In future, it can place different kind of element particle into specific location respectively. So it is important to know the attachment of these two kinds of element particle. Chapter 4.2 has introduced the attachment of P30 particle in PB solution. This chapter will introduce the attachment of pure platinum in DI water.

Here it need to explain something at beginning. The zeta potential of pure gold particle and pure platinum particle are similar, we measure the zeta potential of these two kinds of particle by machine shows the result are nearly same. It is means when processing particle placement the pure gold particle and pure platinum particle are hardly distinguish. And this is another reason we fabricate P30 by coating pure gold with probe DNA. P30 have much high zeta potential than pure gold due to the p-DNA is negative charged. In another word P30 will suffer much high repulsive force in solution than pure gold and we use this method to distinguish gold particle and platinum particle. What is

more, pure gold particle or pure platinum particle can aggregate when they in salt solution. That means we cannot control the particle placement condition via change the ion concentration or solution pH. In fact, pure gold was proven to aggregate in 0.01mM PB solution which contain very low ion concentration. Same thing will happen as pure platinum particle. However if we use P30 particle which have much high zeta potential, it can survives in PB solution. The follow Figure 4-9, Figure 4-10 and Figure 4-11 display the zeta potential of pure gold particle, pure platinum particle and P30 particle respectively.

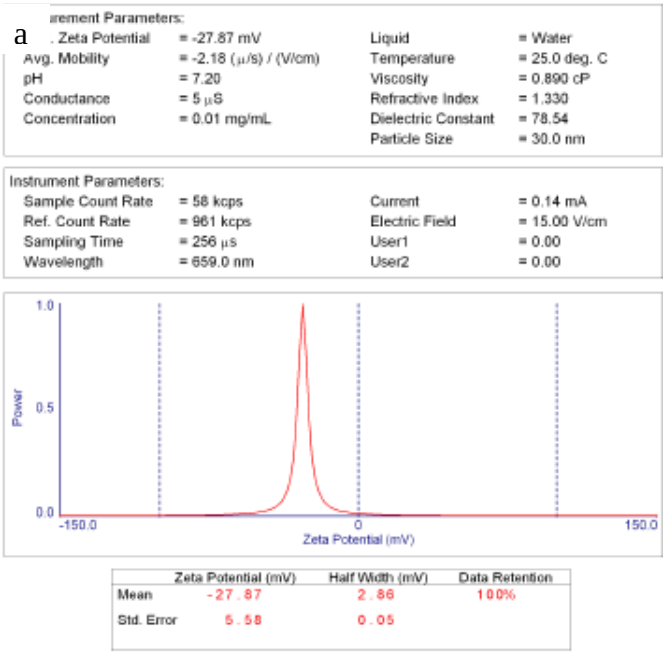

Figure 4-9 Zeta potential of pure gold particle

b

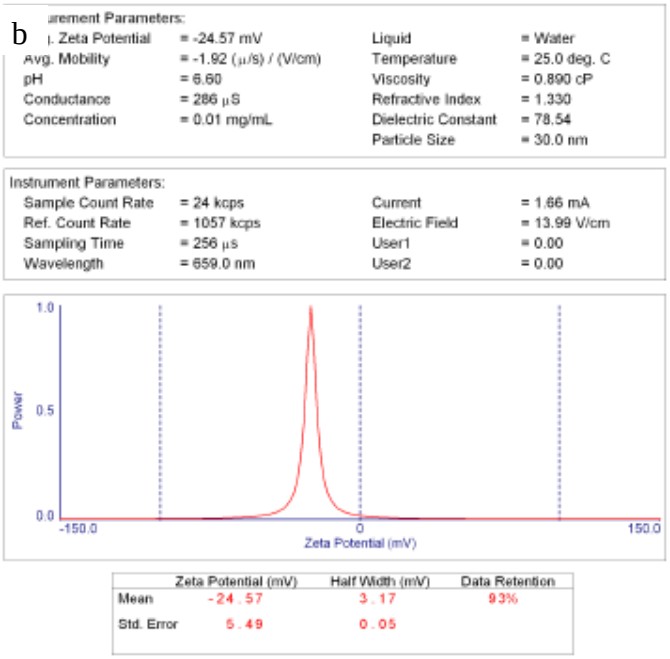

Figure 4-10 Zeta potential of pure platinum particle

c

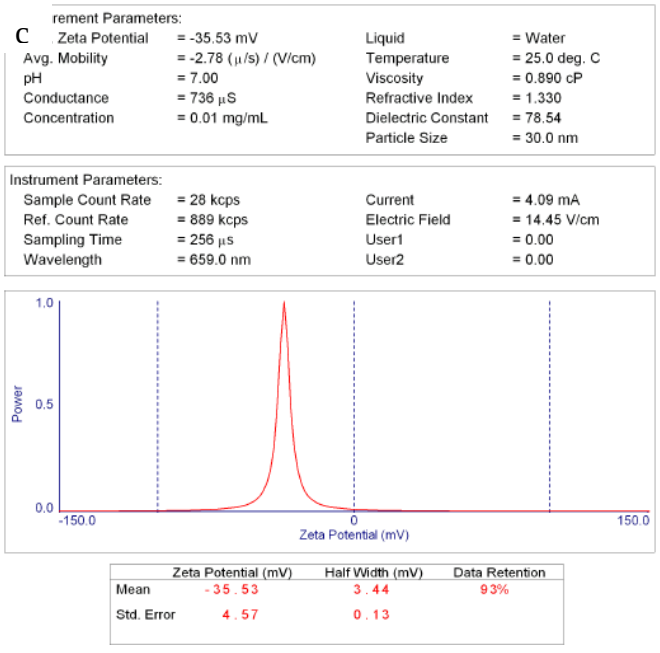

Figure 4-11 Zeta potential of P30 particle

It can make a table to display the difference among pure gold in DI water, pure platinum are in DI water and P30 in TE buffer. See Table 4-4. Zeta potential of pure gold particle is -27.9mv while the zeta potential of P30 particle is -35.5mv. It also proves that, P30 is stable in PB solution and we can vary ionic concentration and solution pH to change P30 zeta potential further.

Table 4-4 Zeta potential of particle

	Particle density (mg/mg)	PH	Zeta potential (mv)
Pure gold	0.01	7.2	-27.9
Pure platinum	0.01	6.6	-24.6
P30	0.01	7	-35.5

Due to the low zeta potential of pure platinum particle, user can choose DI water as solvent to process particle placement experiment. In one way, DI water will increase the particle zeta potential because of low concentration; but without DNA coating the platinum particle has low negative charge than P30 particle in other way. So we cannot judge which particle have better attachment condition without experiment. The experimental temperature is around 25°C. The viscosity of DI water is low than PB solution.

The Figure 4-10 displays the pure platinum placement condition on silicon blank wafer. To observe clearly, we increase the magnification twice at 60KX. The red frames in figure are $0.04um^2$ square and can use to count the particle density of sample. Around 26 particles in the square of Figure 4-10 and the density is $6/0.04=150/um^2$.

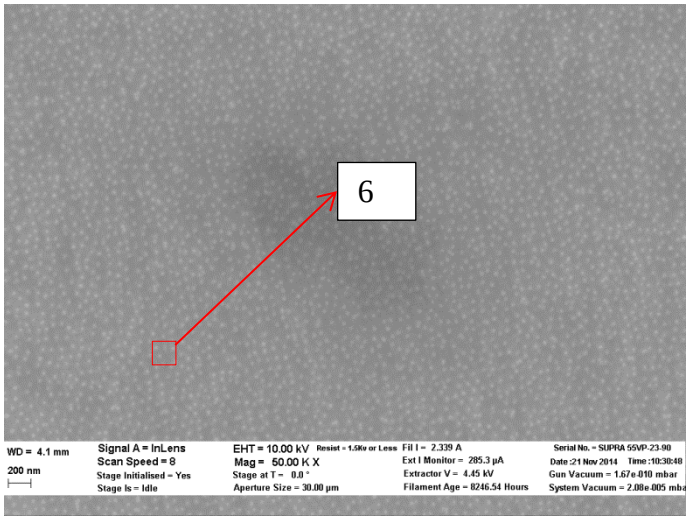

Figure 4-12 Pure platinum particle placement condition in blank Si wafer

By comparing the Figure with Figure 4-1 which is the P30 particle placement condition on blank Si wafer, it can know the pure platinum particle in DI water have much higher density of placement 150/ um^2 than P30 particle in PB solution. (0.1mM PB solution placement density = 56 um^2 and 0.01mM PB solution placement density = 27 um^2.)

The Figure 4-11 displaces the pure platinum particle placement condition in different size of holes. The holes for pure platinum particle are smaller than the holes for P30 particle overall by considering pure platinum particle has less negative charge. The diameters of holes were designed on Auto-CAD range from 90nm to 200nm. (The diameter will increase in real pattern). It can see Figure 4-11 the pure platinum particles become enter into the holes when the holes' diameter less than 200nm compare with P30 in 0.1mM PB solution pH=7 (only one of eight particle enter into the 220nm holes.) So it can roughly think that when the holes' sizes are same, the pure platinum particles are easy to enter into holes than P30 particles in 0.1mM PB solution.

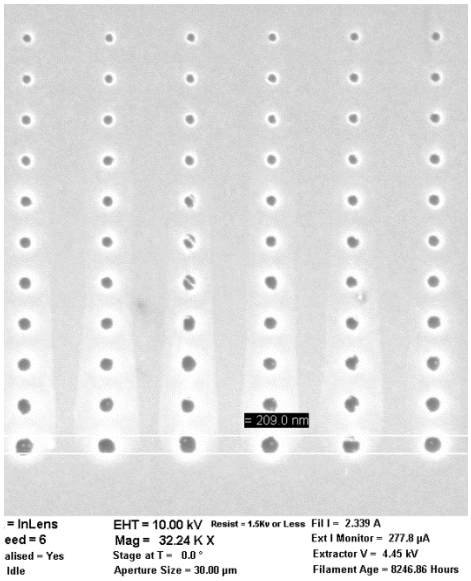

Figure 4-13 Pure platinum particle placement condition with pattern

It can find other interested thing is although the pure platinum particle in DI water, the density of placement condition without pattern is high than P30 in 0.1mM PB solution pH=7, the platinum particle placement condition with pattern is similar as P30 particle. The reason is when particle surface potential decrease, both attractive and repulsive electrostatic force between particle and template surface will. The particle cannot perceive enough attractive electrostatic force to enter into the holes. However, when increase the particle surface potential by decrease the ion strength, compare the data of pure platinum particle and the data of P30 in 0.05mM PB pH=7 the former attachment is much better both in blank wafer and pattern. In this condition, if we place P30 particle in 0.05mM PB solution pH=7 first then place pure platinum particle later we can distinguish these two kinds of particle easily. Because pure platinum particle in DI water can more easily enter into the hole than P30 particle in 0.05mM PB solution pH=7.

Figure 4-12 display the pure platinum particle place in “Pt” and “Au” pattern. It is shows that platinum particle begin to enter into hole when D (diameter of hole) =170nm.

Platinum particle can almost fill the holes when D over 207nm. Compare with P30 particle placement condition in 0.01mM PB solution pH=7. P30 particle begin enter into hole when D=220nm; and it can almost filled holes when D over 270nm. So the thesis design the pattern like this: template has two kinds of holes (1) D=210nm and (2) D=280nm, then we place P30 particles in 0.05mM PB solution pH=7 first, according to the experiment data they will fill the D=280nm holes but cannot enter the D=210nm holes. Then place pure platinum particles in DI water the platinum particle can fill the rest (D=210nm) holes but not D=280nm holes according to Chapter 1.2.

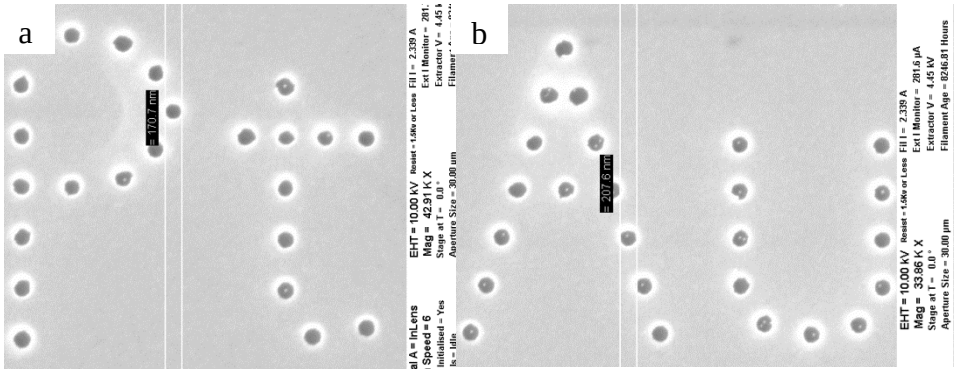

Figure 4-14 (a) Pure platinum particle placement condition with “Pt” pattern (b) Pure platinum particle placement condition with “Au” pattern

In conclusion, pure platinum particle have low negative charge and zeta-potential than P30 particle. So, pure platinum particle is easier to enter into the hole than P30 particle with the same size. It can use this property to place different element particle in different location respectively.

4.3 Positive resist basic sample

In our experiment, we use two kinds of template. (1) Negative resist basic template (2) Positive resist basic sample. In this Chapter we display some data of particle placement on positive resist basic template and do some discussion.

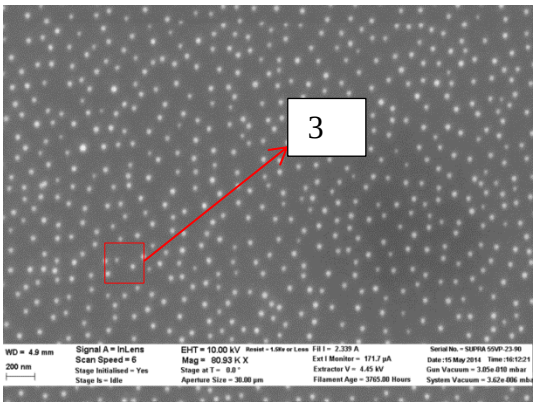

Figure 4-15 P30 particle placement condition in 0.1mM PB solution pH=7 silicon wafer

Figure 4-13 shows the P30 particle placement condition in 0.1mM PB solution pH=7, SEM magnification around 80kX. The area of red square equal to 0.04um^2 and contain 3 particles in square, so the density of particle is 3/0.04=75/um^2. It is close to negative resist basic template56/um^2 with template condition. According to this, the ability of particle placement in positive resist template almost the same as negative resist basic sample.

Figure 4-14 and 4-15 show the P30 particle placement condition in 0.1mM PB solution pH=7 and pure platinum particle placement condition in DI water respectively. From these two pictures we can see the pure platinum particle have better attachment condition than P30 particle. And Figure 4-14 the pure platinum get the ideal particle placement condition: each hole has one particle.

In conclusion, positive resist basic template is easy to make and the pattern are more stable when develop process than negative resist basic sample. However, it cannot make “Pt” and “Au” pattern on it easily. So we didn’t spend much time on positive resist basic sample.

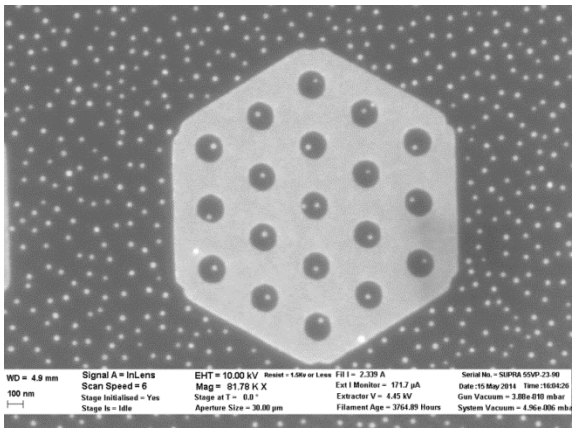

Figure 4-16 P30 in 0.1mM PB solution pH=7 with pattern

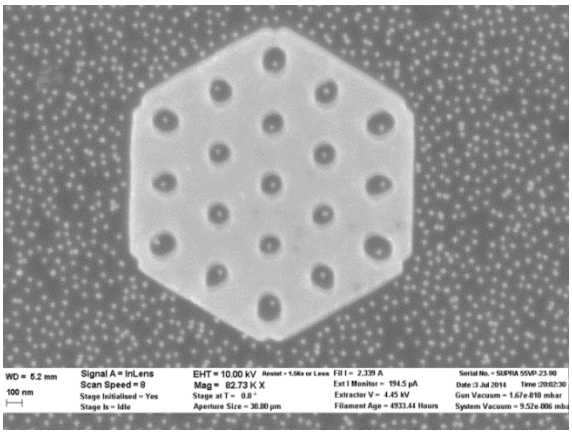

Figure 4-17 Pure platinum particle in DI water with pattern

Chapter 5

Conclusion

This thesis investigated the effect of three parameters on the effectiveness of the single-particle placement (SPP). The three parameters were 1) nanoparticle surface charge, 2) ion concentration of the nanoparticle colloid, and 3) the pH of the nanoparticle colloid. The major results of this thesis can be summarized as follows:

1. The nanoparticle surface charge was controlled by attaching single-stranded DNA molecules to the nanoparticle surfaces and the zeta potential of the resulting DNA-conjugated Au nanoparticles was measured to be -35 mV. The increased negative charges of the DNA-loaded Au nanoparticles prevented nanoparticle agglomeration in the varying ion concentrations and pH's explored in this thesis.

2. The effect of ion concentrations on the SPP was investigated in the ion concentration range of 0.01 mM-0.1 mM at pH 7.0. The effectiveness of the SPP was quantitatively measured with varying sizes of the circular templates and defining the critical diameter, below which no nanoparticles can enter the circular template. The critical diameters were measured to be 210 nm, 250 nm and 280 nm for the ion concentrations of 0.1 mM, 0.05 mM and 0.01 mM, respectively. The increasing critical diameter with decreasing ion concentration was attributed to the increasing Debye length with decreasing ion concentration.

3. The effect of pH on the SPP was investigated in the pH range of 7.0 – 8.0 with an ion concentration of 0.05 mM. The measured critical diameters were 250 nm, 270 nm and 320 nm for pH of 7.0, 7.5 and 8.0, respectively. The increasing critical diameters with increasing pH's were attributed to the increasing deprotonation

(*i.e.*, increasing negative charges) of the carboxyl terminated MHA SAMs ($-COO^-$) on the patterned Au substrate with increasing pH's.

4. The critical parameters of the SPP can be tuned with appropriate combinations of nanoparticle surface charge, ion concentrations of the nanoparticle colloid and pH of the nanoparticle colloid.

References

[1] Klein, D. L. Roth, R.; Lim, A. K. L. Alivisatos, A. P. McEuen, *A single-electron transistor made from a cadmium selenide nanocrystal*. P. L Nature 1997, **389**, 699-701.

[2] Alivisatos, *The use of nanocrystals in biological detection*. P. Nat. Biotechnol. 2004, **22**, 47-52.

[3] Fan, H. Y.; Yang, K.; Boye, D. M.; Sigmon, T. Malloy, K. J.; Xu, H. F. Lopez, G. P. Brinker, *Synthesis of organo-silane functionalized nanocrystal micelles and their self-assembly* C. J. Science 2004, **304**, 567-571.

[4] Chen, J. Perebeinos, V.; Freitag, M. Tsang, J.; Fu, Q.; Liu, J, Avouris, *Bright infrared emission from electrically induced excitons in carbon nanotubes.* P. Science 2005, **310**, 1171-1174.

[5] Heinze, S. Tersoff, J. Martel, R. Derycke, V. Appenzeller, J. Avouris, *Electrically induced optical emission from a carbon nanotube FET.* P. Phys. ReV. Lett. 2002, **89**, 106801.

[6] Tans, S. J. Verschueren, A. R. M. Dekker. *Carbon nanotube intramolecular junctions.* C. Nature 1998, **393**, 49-52.

[7] Huang, Y. Duan, X. Cui, Y. Lauhon, L. J. Kim, K.-H. Lieber. *High performance silicon nanowire field effect transistors*, C.M. Science 2001, **294**, 1313-1317.

[8] Wang, J. Gudiksen, M. S. Duan, X. Cui, Y. Lieber, *Gallium nitride-based nanowire radial heterostructures for nanophotonics*. C. M. Science 2001, **293**, 1455-1457.

[9] Duan, X. Huang, Y. Cui, Y. Wang, J. Lieber, *Single-nanowire electrically driven lasers* , C. M. Nature 2001, **409**, 66-69.

[10] Duan, X. Huang, Y. Agarwal, R. Lieber, *Scalable interconnection and integration of nanowire devices without registration,* C. M. Nature 2003, **421**, 241-245.

[11] Cui, Y. Lieber*, Controlled growth and structures of molecular-scale silicon nanowires*, C. M. Science 2001, **291**, 851-853.

[12] Favier, F. Walter, E. C.; Zach, M. P. Benter, T. Penner, *Individually addressable conducting polymer nanowires array.* R. M. Science 2001, **293**, 2227-2231.

[13] Smith, P. A. Nordquist, C. D. Jackson, T. N.; Mayer, T. S.; Martin, B. R. Mbindyo, J. Mallouk, *Electrochemical synthesis of multi-material nanowires as building blocks for functional nanostructures.* T. E. Appl. Phys. Lett. 2000, **77**, 1399-1401.

[14] Zhang, Y. Chang, A. Cao, J. Wang, Q. Kim, W. Li, Y. Morris, N. Yenilmez, E. Kong, J. Dai, *Efficient formation of iron nanoparticle catalysts on silicon oxide by hydroxylamine for carbon nanotube synthesis and electronics.* H. Appl. Phys. Lett. 2001, **79**, 3155-3157.

[15] Wang, Y. H. Maspoch, D.; Zou, S. L. Schatz, G. C. Smalley, R.E. Mirkin, *Generation of Metal Photomasks by Dip Pen Nanolithography* C. A. Proc. Natl. Acad. Sci. U.S.A. 2006, **103**, 2026-2031.

[16] Demers, L. M. Ginger, D. S. Park, S. J.; Li, Z. Chung, S. W. Mirkin, *Top Down Meets Bottom Up: Dip Pen Nanolithography and DNA Directed Assembly of Nanoscale Electrical Circuits.* C. A. Science 2002, **296**, 1836-1838.

[17] Cui, Y. Bjork, M. T. Liddle, J. A. Sonnichsen, C. Boussert, B. Alivisatos, *Surface-functionalized CdSe nanorods for assembly in diblock copolymer templates.*
A. P. Nano Lett. 2004, **4**, 1093-1098.

[18] Xia, Y. N. Yin, Y. D. Lu, Y. McLellan, *Ordered metal nanoshell materials*. J. AdV. Funct. Mater. 2003, **13**, 907-918.

[19] Nicewarner-Pena, S. R. Freeman, R. G. Reiss, B. D.; He, L. Pena, D. J. Walton, I. D. Cromer, R.; Keating, C. D. Natan, *Photochemical synthesis of gold nanorods*. M. J. Science 2001, **294**, 137-141.

[20] Park, S. J. Taton, T. A. Mirkin, *Multicomponent magnetic nanorods for biomolecular separations*. C. A. Science 2002, **295**, 1503-1506.

[21] H. W. Huang, P. Bhadrachalam, V. Ray and S. J. Koh, *Single-particle placement via self-limiting electrostatic gating.* Appl.Phys. Lett., 2008, **93**, 073110–073113.

[22] Moshood K. Morakinyo, Shankar B. Rananavare*. Reducing the effects of shot noise using nanoparticles.* J. *Mater.* Chem. C, 2015, **3**, 955–959.

[23] Menachem Elimelech, William H. Chen, John J. Waypa. *Measuring the zeta (electrokinetic) potential of reverse osmosis membranes by a streaming potential analyzer*. Desalination Volume **95**, Issue 3, July 1994, Pages 269–286.

[24] Robert J. Hunter Zeta Potential in Colloid Science: *Principles and Applications Academic.* Press, Sep 3, 2013 Science 398 pages.

[25] Laurent Nachbaura, Pierre-Claver Nkinamubanzib, André Nonata, Jean-Claude Mutina. *Electrokinetic Properties which Control the Coagulation of Silicate Cement Suspensions during Early Age Hydration*. J. Colloid Interface Sci. **202** (1998), pp. 261–268.

[26] Hélène Viallis-Terrissea, André Nonatb, Jean-Claude Petita. *Zeta-Potential Study of Calcium Silicate Hydrates Interacting with Alkaline Cations*. J. Colloid Interface Sci. **244** (2001), pp. 58–65.

[27] Ryszard Sprycha Electrical double layer at alumina/electrolyte interface: I. *Surface charge and zeta potential.* Journal of Colloid and Interface Science Volume **127**, Issue 1, January 1989, Pages 1–11.

[28] Eighth CANMET/ACI International Conference on Superplasticizers and Other Chemical Admixtures in Concrete, Sorrento (Italy), SP 239-16 (2006), pp. 231–248

[29] Marshall Fixman, *Thin double layer approximation for electrophoresis and dielectric response*. J. Chern. Phys. **78**(3), 1 Feb. 1983.

[30] Byung Jun Yoon, *Sangtae Kim Electrophoresis of spheroidal particles*. Journal of Colloid and Interface Science Volume **128**, Issue 1, 1 March 1989, Pages 275–288.

[31] John A. Schellman*. Electrical double layer, zeta potential, and electrophoretic charge of double-stranded DNA.* Biopolymers. Volume **16**, Issue 7, pages 1415–1434, July 1977

[32] Ursula Schnabel, Christian-Herbert Fischer, Ernst Kenndler. *Characterization of Colloidal Gold Nanoparticles According to Size by Capillary Zone Electrophoresis*. J. Microcolumn Separations, **97** , 529.

[33] Krieger M, Scott MP, Matsudaira PT, Lodish HF, Darnell JE, Lawrence Z, Kaiser C, *Berk Approximate methods of determining the double-layer free energy of interaction between two charged colloidal spheres*. Journal of Colloid and Interface Science. Volume **33**, Issue 3, July 1970, Pages 335–359.

[34] Richard R. *Sinden DNA Structure and Function Elsevier*, Dec 2, 2012 Science, 398 pages.

[35] Ming Zheng, *Structure-Based Carbon Nanotube Sorting by Sequence-Dependent DNA Assembly.* Science 28 November 2003: Vol. **302** no. 5650 pp. 1545-1548

[36] Daniela Zanchet, Christine M. Micheel, Wolfgang J. Parak, Daniele Gerion, A. Paul Alivisatos. *Electrophoretic Isolation of Discrete Au Nanocrystal/DNA Conjugates*. Nano Lett., Vol. **1**, No. 1, 2001.

[37] Angel S. Butron, *DNA-Functionalized Gold Nanoparticles as Probes in Biomolecule Detection Assays*, Volume **4**, Issue 1, Summer 2007 Nanoscape.

[38] Christine Schwer , Ernst Kenndler, *Electrophoresis in fused-silica capillaries: the influence of organic solvents on the electroosmotic velocity and the zeta Potential*. *Anal. Chem.*, 1991, **63** (17), pp 1801–1807.

[39] Leland M. Vane. *Effect of aqueous phase properties on clay particle zeta potential and electro-osmotic permeability: Implications for electro-kinetic soil remediation*

processes. Journal of Hazardous Materials. Volume **55**, Issues 1–3, August 1997, Pages 1–22.

[40] M.G. Carneiro-da-Cunha et al. *Influence of concentration, ionic strength and pH on zeta potential and mean hydrodynamic diameter of edible polysaccharide solutions envisaged for multinanolayered films production*. Carbohydrate Polymers **85** (2011) 522–528.

[41] Douglas B. Burns, Andrew L. Zydney. *Buffer effects on the zeta potential of ultrafiltration membranes.* Journal of Membrane Science. Volume **172**, Issues 1–2, 1 July 2000, Pages 39–48.

[42] Richard W. O. Brien, *Lee R. White Electrophoretic mobility of a spherical colloidal particle.* J. Chem. Soc., Faraday Trans. 2, 1978, **74**, 1607-1626

[43] Shaw, D.J. (1992) *Introduction to Colloid and Surface Chemistry*, Butterworth Heinemann, UK.

[44] Bruce Alberts, Glenn Herrick, *DNA-cellulose chromatography.* Methods in Enzymology. Volume **21**, 1971, Pages 198–217.

[45] M. Ageno, E. Dore. *The alkaline denaturation of DNA*. Physics Laboratory, Istituto Superiore di Sanita, Rome, Italy.

[46] Z.Q. Wei, C. Wang, C.F. Zhu, C.Q. Zhou, B. Xu, C.L. Bai. *Study on single-bond interaction between amino-terminated organosilane self-assembled monolayers by atomic force microscopy Surface Science*. Volume **459**, Issue 3, 10 July 2000, Pages 401–412.

[47] Shihua Song , Rose A. Clark , Edmond F. Bowden , Michael J. Tarlov. *Characterization of cytochrome c/alkanethiolate structures prepared by self-assembly on gold*. *J. Phys. Chem.*, 1993, **97** (24), pp 6564–6572.

[48] Fei Huang, Song Qu, Song Zhang, Baohong Liu, Jilie Kong. *Sensitive detection of clozapine using a gold electrode modified with 16-mercaptohexadecanoic acid self-assembled monolayer*. Talanta Volume **72**, Issue 2, 30 April 2007, Pages 457–462.

[49] D. A. Bryant, *Debye length in a kappa-distribution plasma. Journal of Plasma.* Physics, Volume **56**, Issue 01, August 1996, pp 87- 93.

[50] Rafael Tadmor, Ernesto Hernández-Zapata, Nianhuan Chen, Philip Pincus, Jacob N. Israelachvili. *Debye Length and Double-Layer Forces in Polyelectrolyte Solutions.* Macromolecules, 2002, **35** (6), pp 2380–2388.

[51] Dr. Isaac Klapper1, Ray Hagstrom1, Richard Fine2, Kim Sharp3 and Dr. Barry Honig. *Focusing of electric fields in the active site of Cu-Zn superoxide dismutase: Effects of ionic strength and amino-acid modification. Proteins: Structure, Function, and Bioinformatics*. Volume **1**, Issue 1, pages 47–59, January 1986.

[52] Dongqing Li. *Electrokinetics in Microfluidics*. Academic Press, Aug 20, 2004 Technology & Engineering 652 pages.

[53] Norihiro Inagaki. *Plasma Surface Modification and Plasma Polymerization*. CRC Press, Mar 6, 1996 Technology & Engineering 265 pages.

[54] Jiwen Zheng, Zihua Zhu, Haifeng Chen and Zhongfan Liu. *Nanopatterned Assembling of Colloidal Gold Nanoparticles on Silicon*. Langmuir, 2000, **16** (10), pp 4409–4412.

[55] Hiroto Miyakea, Shen Yea, b, Masatoshi Osawa. *Electroless deposition of gold thin films on silicon for surface-enhanced infrared spectroelectrochemistry*. Electrochemistry Communications Volume **4**, Issue 12, December 2002, Pages 973–977.

[56] Y.J. Xing, D.P. Yu, Z.H. Xi, Z.Q. Xue. *Silicon nanowires grown from Au-coated Si substrate*. Applied Physics A March 2003, Volume **76**, Issue 4, pp 551-553.

[57] S Zankovych, T Hoffmann, J Seekamp, J-U Bruch, C M Sotomayor Torres. *Nanoimprint lithography: challenges and prospects.* Nanotechnology **12** (2001) 91–95

[58] Ki Hyun Bae, Seung Ho Choi, Sung Young Park, Yuhan Lee, Tae Gwan Park. *Thermosensitive Pluronic Micelles Stabilized by Shell Cross-Linking with Gold Nanoparticles.* Langmuir, 2006, **22** (14), pp 6380–6384.

[59] Chung-Wei Chang, Wei-Lung Tseng. *Gold Nanoparticle Extraction Followed by Capillary Electrophoresis to Determine the Total, Free, and Protein-Bound Aminothiols in Plasma.* Anal. Chem., 2010, **82** (7), pp 2696–2702.

[60] Yanbing Zu Zhiqiang Gao. *Facile and Controllable Loading of Single-Stranded DNA on Gold Nanoparticles.* Anal. Chem, 2009, **81** (20), pp 8523–8528.

[61] Gang Han et al. *Light-Regulated Release of DNA and Its Delivery to Nuclei by Means of Photolabile Gold Nanoparticles*. Angewandte Chemie Volume **118**, Issue 19, pages 3237–3241, May 5, 2006.

Biographical information

KunHua Yu was born on GuiZhou, China on August 27 1990. He received his B.S degree in engineering from the Harbin Institute of Technology, China in June 2013. Then he came to America for his M.S. degree in September 2013. He worked for Doc. Seong Jin Koh as research assistant and his project involved Studying the effect of ion concentration, pH, and surface charge on particle placement. During 2013 to 2015, his GPA was 3.8. He received the 2013 department graduate scholarship on both 2013 and 2014.